Step Location Control to Overstep Obstacles for Running Robots

ing. S.N. van der Geld

Master of Science Thesis

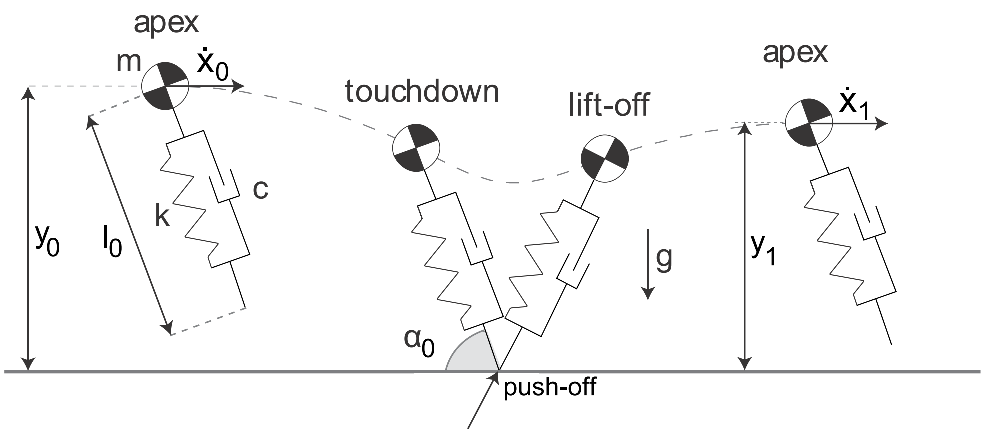

Delft University of Technology

Faculty of Mechanical, Maritime and Materials Engineering

Step Location Control to Overstep Obstacles for Running Robots

Master of Science Thesis

For the degree of Master of Science in Mechanical Engineering at Delft University of Technology

ing. S.N. van der Geld

June 21, 2012

Faculty of Mechanical, Maritime and Materials Engineering · Delft University of Technology

Delft University of Technology
Department of
BioMechanical Design

The undersigned hereby certify that they have read and recommend to the Faculty of Mechanical, Maritime and Materials Engineering for acceptance a thesis entitled

Step Location Control to
Overstep Obstacles for
Running Robots

by

ing. S.N. van der Geld

in partial fulfillment of the requirements for the degree of

Master of Science Mechanical Engineering

Dated: June 21, 2012

Supervisor: ______________________
ir. J.G.D. Karssen

Readers: ______________________
prof.dr. F.C.T. van der Helm

____
dr.ir. M. Wisse

____
dr.ir. M. Langelaar

Table of Contents

Chapter 1

Step Location Control to Overstep Obstacles for Running Robots

Step Location Control to Overstep Obstacles for Running Robots

Delft Biorobotics Laboratory, Mechanical Engineering, Delft University of Technology
S.N. van der Geld, Advisor: J.G.D. Karssen,
June 7, 2012

***Abstract*—Obstacles in the path of a running robot need to be avoided in order to avoid falling down. Currently, there are no control strategies that determine the appropriate step locations to obtain a successful overstep of an obstacle. The objective of this simulation study is to maximize the gap size by determining the step locations. The step strategy is tested on the SLIP-model and a model containing leg damping and push-off. With the means of an optimization, it is found that the optimal step strategy consists out of 3 phases: an adaptive phase from running cycle to the optimal state for the beginning of the leap, the beginning and end of the leap and another adaptive phase to end in a desired end state. For the SLIP-model is found that the maximum gap size is almost independent of the initial velocity of the model and mostly depends of the system's energy. In order to maximize the gap size, the first and second step location have to be coincident. Furthermore, the damping and push-off proved to be an important factor for the step locations and the obtained gap size, as the first and second step locations do not coincident anymore and the gap size is reduced significantly.**

***Index Terms*—Robotics, SLIP, step location, maximum gap size**

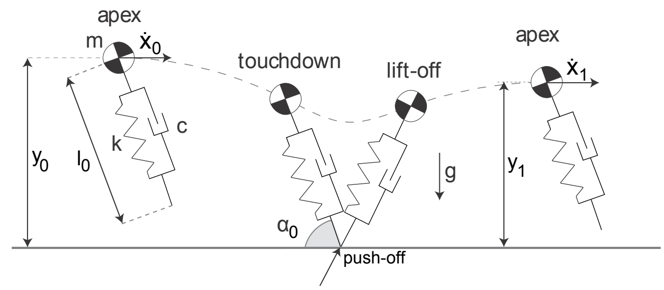

Fig. 1. The Damped Spring Loaded Inverted Pendulum (DSLIP) model, this model differs from the standard SLIP-model due to the addition of the damper. The model consists of a point mass m, attached to a massless linear spring, with spring constant k and rest length l_0. Parallel to the spring is a damper fitted with damping constant c, which functions like a simple dashpot. The model is subject to gravitational acceleration g. The highest point of the flight phase is called apex. The instances where the foot touches and leaves the ground are called touchdown and lift-off respectively. At lift-off the model pushes-off, which instantaneous adds a fixed amount of energy E_{push}. The angle of the leg with respect to the ground at the moment of touchdown is called the angle of attack, denoted by α_0.

I. Introduction

ALMOST all current mobile robots use wheels to move around. Wheels provide an easy to implement and energy efficient way of moving around, but wheels restrict robots to flat terrain. Legged robots, on the other hand, have the potential to handle non-flat or rough terrain, as they can select their ground contact points. The forward velocity for walking robots is limited to $\sqrt{gl}$ [1] [1], this boundary can be exceeded if the robot starts running. Therefore, a running robot can travel faster than a walking robot and is able to handle not-flat terrain better than a wheeled robot.

Running robots have been built in different shapes and sizes. There are monopods [2–4], bipeds [5–7], quadrupeds [8, 9] and hexapods [10, 11]. The current state-of-art legged bipedal robots are able to walk or run on a flat terrain and they can cope with small perturbations [6, 7, 12]. These robots cannot handle rough terrain though, because they only react to perturbations, which works well if the perturbation is small. However, an anticipative action is needed to handle a larger perturbation.

A large perturbation can be caused by an obstacle in the running trajectory. Obstacles can be avoided by stepping around, stepping on, or stepping over them. Obstacle avoidance has been studied for both humans and for robots. For humans, step location preference has been studied [13–16] and it is shown that humans start to adjust their gait in the last two steps prior overstepping an obstacle [17]. However, an exact step planning strategy is not known yet. In robotics research, stepping around obstacles has been studied extensively [18–25] and for running robots it has been shown how to adjust the running gait in order to select ground contact points [26, 27]. However, there is no strategy to optimize step locations.

In this paper we focus on overstepping an obstacle and we omit stepping around or on obstacles. This leads to a strategy which can be applied for both 2D as 3D simulations and for obstacles or gaps. In order to avoid the influences of obstacle height to the step locations, only gap size is studied. Further, this study focuses on how to overstep a gap, hence the location of the gap itself is omitted. The goal of this study is defined as: *"To determine step locations for running robots in order to overstep the largest gap possible."*

In order to overstep a gap, it has to be determined where a bipedal robot can place its feet without falling down. Pratt et al. [28] proposed a method for walking robots to determine step locations for which the robot can come to a full stop in N-steps. We show that the behavior of running robots compared with walking robots is different, that is why it is not possible to use the method proposed by Pratt et al. to determine step locations for running robots. Therefore, an optimization study is necessary.

[1] in which l is the leg length and g is the gravitational acceleration

The goal of this study is achieved by the means of a simulation study, for which an optimization is implemented. In this paper, a method to maximize the gap size is presented and this method is used to determine the optimal step locations for the DSLIP-model. This model is an expanded version of the SLIP-model with a damper and push-off.

The remainder of this paper is organized as follows. Section II introduces the simulation model used in this study. Section III discusses the method used to determine the capture basin of the model. Section IV discusses how to determine the maximum gap size possible. Section V discusses the results obtained with the optimization. Section VI discusses these results and Section VII discusses the conclusions. The recommendations for further research are given in Section VIII.

II. The DSLIP Model

An important 2D model in running robotics is the Spring Loaded Inverted Pendulum (SLIP) model [29]. Although the model is simple, research has shown that running gaits calculated with this model are similar to human and animal running gaits [29], [30]. The SLIP-model consists of a point mass attached to a massless spring. A drawback of the SLIP-model is that it is a conservative model, which does not allow changes in the system energy during the gait. In this study we make the model non-conservative by adding a damper and a push-off at lift-off to the SLIP-model, see Fig. 1. We use this non-conservative model, because we believe that the system energy is an important state in obstacle overstepping. We call this model the Damped Spring Loaded Inverted Pendulum (DSLIP) model.

The motion of the DSLIP-model can be divided into two distinct phases: the flight phase and the stance phase. The behavior of the flight phase of the model is equal to a ballistic motion, leading to the following equations of motion:

$$\begin{bmatrix} \ddot{x} \\ \ddot{y} \end{bmatrix} = \begin{bmatrix} 0 \\ -g \end{bmatrix}, \tag{1}$$

in which $\ddot{x}$ and $\ddot{y}$ are respectively the horizontal and vertical acceleration of the point mass and g is the gravitation acceleration. During the stance phase, the motion of the point mass is affected by the leg forces F_s and F_d and by the gravitational acceleration:

$$\begin{bmatrix} \ddot{x} \\ \ddot{y} \end{bmatrix} = \begin{bmatrix} -\cos\alpha \\ \sin\alpha \end{bmatrix} \frac{F_s + F_d}{m} + \begin{bmatrix} 0 \\ -g \end{bmatrix}, \tag{2}$$

in which F_s and F_d are the forces in the spring and the damper respectively, m is the mass of the point mass and α is the angle between leg spring and ground. In this study, we use a linear spring and a damper which is proportional to its velocity. The damper only functions when the leg is compressing to ensure that lift-off only occurs at the rest length of the leg spring. The leg forces are given by:

$$\begin{aligned} F_s &= k(l - l_0) \\ F_d &= \begin{cases} c\dot{l}, & \dot{l} < 0 \\ 0, & \dot{l} \geq 0 \end{cases}, \end{aligned} \tag{3}$$

TABLE I
DSLIP MODEL PARAMETERS

Parameter	Symbol	Value	Unit
mass	m	1	kg
leg length	l_0	1	m
gravity	g	1	$\frac{m}{s^2}$
spring constant	k	22.8	$\frac{N}{m}$
damping constant	c	4.6	$\frac{Ns}{m}$
push-off energy	E_{push}	0.1	J

in which k and c are the spring and damper constant respectively, l is the spring length, $\dot{l}$ is the leg velocity and l_0 is the length of the spring at rest.

The damper dissipates energy, hence energy needs to be added in order to return to the initial conditions of the model. The energy is added with an impulsive push-off at the end of the stance phase. The push-off is applied in the direction of the leg and causes an instantaneous velocity change Δv:

$$\begin{bmatrix} \dot{x}^+ \\ \dot{y}^+ \end{bmatrix} = \begin{bmatrix} \dot{x}^- \\ \dot{y}^- \end{bmatrix} + \begin{bmatrix} -\cos\alpha \\ \sin\alpha \end{bmatrix} \Delta v, \tag{4}$$

in which $\dot{x}^-$ and $\dot{y}^-$ are the horizontal and vertical velocity respectively before push-off and $\dot{x}^+$ and $\dot{y}^+$ are the horizontal and vertical velocity after the push-off. The magnitude of the push-off is set such that the energy supplied by the push-off E_{push} is constant:

$$\begin{aligned} E^+ &= E^- + E_{push} \\ \tfrac{1}{2}m\left(\dot{x}^{+2} + \dot{y}^{+2}\right) &= \tfrac{1}{2}m\left(\dot{x}^{-2} + \dot{y}^{-2}\right) + E_{push} \end{aligned} \tag{5}$$

The stance and flight phases alternate each other by a switching moment. The transition from flight phase to stance phase is called touchdown. This happens when the foot hits the ground:

$$y = l_0 \sin\alpha_0 , \tag{6}$$

in which the angle α_0 is the angle between leg spring and ground at touchdown, also called the angle of attack. The transition from stance phase to flight phase is called lift-off. This happens when the foot leaves the ground, which is when the leg spring returns to its rest length. This moment can be denoted by:

$$\begin{aligned} l &= l_0 \\ \dot{l} &> 0 \end{aligned} \tag{7}$$

The state of the DSLIP-model is described by four inputs: the horizontal and vertical positions x and y and the horizontal and vertical velocities $\dot{x}$ and $\dot{y}$. The model is completely described by the height y and the horizontal velocity $\dot{x}$ at the highest point of the flight phase, called the apex. As the vertical velocity is zero at this point by definition and the horizontal position is irrelevant for normal running motion of the model. This reduces the input state of the model at apex to

$q_0 = [y_0\ \dot{x}_0]^T$. In this study, we choose to set the energy level of the DSLIP-model to be constant, therefore the initial state is set to $q_0 = [E_0\ \dot{x}_0]^T$ in which E_0 the initial energy level is. The initial height of the system at apex is defined as:

$$y_0 = \frac{E_0 - \frac{1}{2}m\dot{x}_0^2}{mg} \tag{8}$$

In this study, a normalized model is used in order to obtain results which are only dependent of the characteristics of the model behavior. Therefore, all length and mass values are set to unit length and mass. The normalized spring constant k is based on the spring stiffness in the running robot Phides [31] and is not varied in this study. The spring constant k is normalized by:

$$k = \frac{k_{robot}L_{0(robot)}}{m_{robot}g}\ , \tag{9}$$

in which k_{robot}, m_{robot} and $L_{0(robot)}$ are the spring constant, the mass and the leg length of the robot Phides respectively.

Raibert et al. [32] reported a mechanical loss of 25% hopping energy per step for their bipedal hopping robot. The same percentage of energy loss per step is used in this simulation study. We use the kinetic energy at touchdown to determine the loss per step. The damping constant c and push-off energy E_{push} are determined for a limit cycle run with a velocity of 2 m/s. This velocity is chosen such that it is necessary to run, as it exceeds the maximum walking velocity [1]. The damping constant and push-off energy are held constant for the rest of this study. For calculations without damping and added push-off energy, the SLIP-model is used. The parameters used in this study are given in Table I.

III. Capture Point and Capture Regions

It is useful to know which step locations will not cause the robot to fall down. These step locations can be used to determine a strategy to overstep an obstacle. Pratt et al. [28] proposed a method for walking robots to determine step locations at which the robot can come to a full stop in N-steps. This method is applied to the Linear Inverted Pendulum Model (LIPM), which is a simplified model for human and robotic walking [33].

The initial velocity and height of the model determine the number of steps in which a full stop can be obtained. The total state space containing these number of steps is called the capture basin. The step location at which standstill is obtained is called the capture point. The capture region is defined as the set of step locations at which stepping is possible and where standstill can be obtained in the next N-step(s). The requirement of being able to come to a stop is essential, as being able to take N-steps more, but eventually falling down and not achieving standstill is considered as falling down.

The SLIP and DSLIP-model are nonlinear models, whereas LIPM is a linear model. The capture point and capture regions for LIPM can be calculated using linear equations, according to [28] and [34]. Because linear equations are computationally less expensive to solve than nonlinear equations, it is investigated whether LIPM can be used to calculate capture points and regions for SLIP and DSLIP-model based robots.

A. LIPM vs. SLIP and DSLIP Behavior

The LIPM model is a linear model and is in closed form solvable. The equation of motion for the LIPM model is given by:

$$\ddot{x} = \frac{g}{y_0}x, \tag{10}$$

in which $\ddot{x}$ and x are the acceleration and position respectively of the point mass in horizontal direction and y_0 is the constant height of the point mass. The capture point can be derived using equation (10) and a conserved quantity called the Linear Inverted Pendulum Orbital Energy equation [33]. This equation represents the energy a spring-mass system with unit mass and length and a negative stiffness of $-\frac{g}{y_0}$:

$$E_{LIP} = \frac{1}{2}\dot{x}^2 - \frac{g}{2y_0}x^2, \tag{11}$$

and standstill will occur if x and $\dot{x}$ become zero, thus when E_{LIP} is zero. Rewriting equation (11) for $E_{LIP} = 0$ gives the two eigenvectors of the system:

$$\dot{x} = \pm\sqrt{\frac{g}{y_0}} \tag{12}$$

The step location at which standstill will occur can be obtained by rewriting equation (12) for the stable eigenvector:

$$x_{capture} = \dot{x}\sqrt{\frac{y_0}{g}} \tag{13}$$

The capture point for the SLIP and DSLIP-model is defined as the location at which the model will maintain hopping with zero horizontal velocity. Zero horizontal velocity is obtained by choosing the angle of attack such that all of the initial energy in the system is transformed into potential energy at the end of the step. Thus, the angle of attack is chosen such that the input state $q_0 = [E_0\ \dot{x}_0]^T$ is transformed into the end state $q_1 = [E_1\ 0]^T$. By the means of an optimization implemented in MATLAB using the function `fminsearch`, is the angle of attack determined to obtain this desired end state.

The step location at which standstill is obtained is shown in Fig. 2, showing the initial forward velocity $\dot{x}_0$ plotted against the capture point. Both the SLIP as the DSLIP-model behavior is calculated. For the same initial velocity, it can be seen that the capture point location for SLIP and DSLIP-model are almost equal, however they differ from LIPM. There is no capture point for the DSLIP-model for lower initial velocities. The damping dissipates too much energy of the model for the spring to return to rest length. As lift-off is triggered at rest length of the spring, the model keeps its foot on the ground and will not lift-off. The model falls over, ending in a fail state.

It can be concluded that LIPM capture points and regions cannot be used for SLIP and DSLIP based models. As the difference between the SLIP and the DSLIP-model is negligible, the SLIP-model is used to determine the capture point and capture regions.

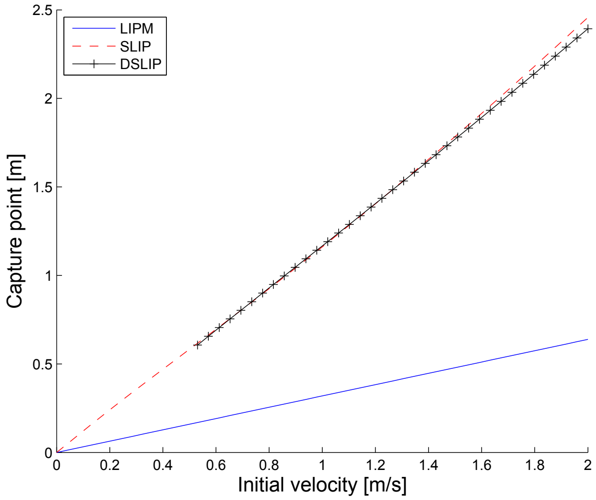

Fig. 2. Capture point location as function of the initial velocity for LIPM, SLIP and DSLIP. The initial conditions for the models are $q_0 = [y_0\ \dot{x}_0]$, with $y_0 = 1\ m$. All three models show, that the location of the capture point moves forward with increasing initial velocity. The graph shows that SLIP and DSLIP have similar capture points and that SLIP and DSLIP disagree with LIPM.

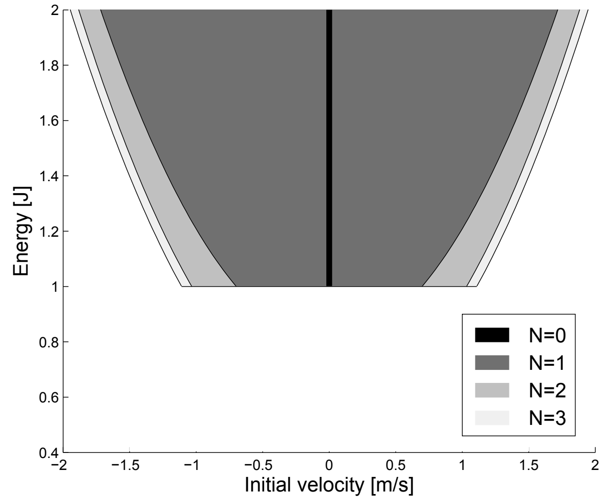

Fig. 3. Capture basin for the SLIP-model. The graph shows depending on the initial conditions, the number of steps in which the robot is able to come to a stop. The lower boundary of the capture basin is given by the minimal energy $E = 1\ J$ for which the model can come to a stop.

B. Capture Basin for SLIP

The capture point and capture regions for the SLIP and DSLIP-model cannot be determined using the method available for LIPM. This section discusses how to determine the capture basin, which is the total state space containing the number of steps the model needs make in order to come to a full stop.

The capture basin is obtained by calculating the speed at the end of one step for an initial speed range $\dot{x}_0$ and range of α_0. By comparing the speed at the end of one step with the initial speed, it can be determined in how many steps the model is capturable. Appendix A explains this process in more detail.

The capture basin is calculated for the SLIP-model and Fig. 3 shows the N-step capturability for the initial conditions. It is shown that the majority of the initial conditions with $\dot{x}_0 \neq 0\ m/s$ will lead to a 1-step capturable system. The model is not capturable for energy levels lower than 1 J, as this is the boundary at which the model can come to a standstill.

The transition between the 1-step and the 2-step boundary and between the 2-step and 3-step boundary is dependent of the initial height. The initial height of the model is bounded by the energy level and the initial velocity, according to equation (8). For a higher initial velocity, the initial height becomes lower until the boundary is reached where the model is unable to come to zero velocity in one step. The lower initial height reduces the possible step locations, as the model is not able to position the leg at all angles in the range of $[0-\pi]$ radians. This makes it necessary take another step. For the 3-step capture basin the same reasoning is valid, as the possible step locations allow the model to take another step, but the end state does not provide a possibility to come to a standstill.

Higher N-step boundaries are not investigated, as these regions are not interesting to step. In Fig. 3 is shown that the capture basin is reduced for higher N-regions. The associated capture regions are also reduced, resulting in a relative small area in which stepping is possible. This is discussed further in Section III-C.

C. Capture Regions for SLIP

The capture regions are the step locations on the ground where the model can stand and at the next apex will be in one of the capture basin regions. Calculating the capture point is useful if a certain point has to be reached, for example stopping before an obstacle. Calculating the capture regions is useful if one wants to keep the robot running and to overstep gaps.

The capture regions can simple be calculated based on the capture basins, because the flight phase behavior of the SLIP-model is equal to a ballistic motion. If the model starts with initial conditions y_0, $\dot{x}_0$, α_0, and l_0, than the height of the foot is given by:

$$h = y_0 - l_0 \sin \alpha_0 \tag{14}$$

The horizontal position of the point mass x_{CoM} depends of the initial velocity and the elapsed time. The horizontal position is given by:

$$x_{CoM} = \dot{x}_0 \sqrt{2h} \tag{15}$$

The horizontal position of the foot is given by the point mass position and the leg length:

$$\begin{aligned} x_f &= x_{CoM} + l_0 \cos \alpha_0 \\ &= \dot{x}_0 \sqrt{2y_0 - \sin \alpha_0} + l_0 \cos \alpha_0 \end{aligned} \tag{16}$$

With the foot location known, the capture regions can be determined. Fig. 4 shows the capture point and regions for the SLIP-model, with the initial velocity range of $\dot{x}_0 = [0-1.2]\ m/s$ and energy level $E = 1.35\ J$. The black line represents

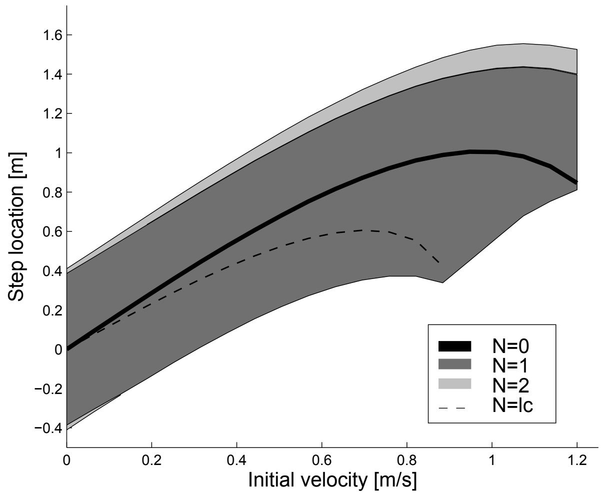

Fig. 4. Capture regions for the SLIP-model. The y-axis represents allowable step locations in which the model is capturable, calculated from the point mass at 0 in m, whereas x-axis represents the initial velocity of the model. The initial energy level is $E = 1.35$ J and the angle of attack range is $[0-\pi]$ radians. The black line represents the capture point at which the model is capturable in $N = 0$ steps. The dark gray area represents the $N = 1$ area, whereas the light gray area represents the $N = 2$ area. The thin black line $(N = lc)$ represents the step location at which limit cycle running is achieved. It shows that for higher initial velocities, the capture region shifts further away from the CoM.

the capture point where standstill occurs denoted by $N = 0$, the dark gray area represents the 1-step capture region with $N = 1$ and the light gray area represents the 2-step capture region at $N = 2$.

If we want robots to overstep a gap, the capture point is not important. Most interesting is the area which allows the robot to put its foot, enabling it to continue running without ending in falling down. Varying the step locations will influence the upcoming step behavior. The range below the capture point line provides step locations for which the robot will maintain forward motion. As can be expected, the step location for limit cycle running lies before the capture point, depictured as the dashed black line $(N = lc)$ below the capture point line $(N = 0)$ in Fig. 4. Stepping in the area between $N = lc$ and the boundary of $N = 1$ will increase forward velocity, whereas stepping in the area between $N = 0$ and $N = lc$ will decrease forward velocity. Stepping beyond the $N = 0$ line will cause the robot to run backwards. For the remainder of this study, the 1-step capture region is the only region taken into account. Because the purpose of this study is to continue running forward after overstepping, the area above the $N = 0$ line and the higher N-regions are neglected, as these regions causes the robot to take another step or to switch direction.

IV. Maximum Gap Size

This section discusses how to use the capture regions calculated in Section III, in order to determine the maximum gap size. The maximum gap size possible depends on the distance between the capture regions of two consecutive steps. In this study, we define the maximum gap as:

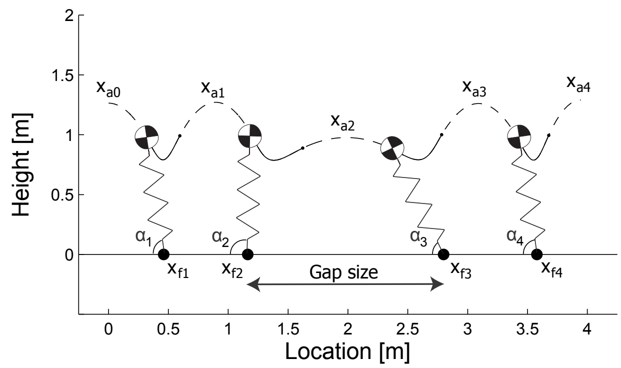

Fig. 5. Trajectory of the SLIP-model. The dashed line shows the trajectory of the point mass during flight phases, whereas the solid line represents the point mass during the stance phases. The SLIP-model is drawn at touchdown for four subsequent steps. In here, α_1, α_2, α_3 and α_4 and x_{f1}, x_{f2}, x_{f3} and x_{f4} are the angles of attack and the step locations of the associated steps respectively. Furthermore, x_{a0}, x_{a1}, x_{a2}, x_{a3} and x_{a4} denote the apexes from start to the end of the step sequence. Finally, 'Gap size' denotes the distance between the 2^{nd} and 3^{th} step location, which is the distance to be maximized.

"The maximum distance between two steps, with the constraint that the robot does not has to put its foot in between these steps in order to prevent falling down."

The constraint prevents the model of putting the upcoming step in between the previous steps, as this effectively shortens the maximum gap size. Fig. 5 shows the SLIP-model drawn for four subsequent steps, this model clarifies the designations used in this en subsequent sections.

Section IV-A discusses the behavior of the model, if for two consecutive steps the boundary of the capture basin is selected and the gap size is determined. We show that the boundaries of the capture basin not necessarily have to lead to the maximum gap size possible. Section IV-B discusses a four step sequence approach to maximize the gap size. We show that using four steps, the maximum gap size can be obtained if the 1^{st} and 2^{nd} step locations and the 3^{rd} and 4^{th} step locations coincide. Moreover, we show that the maximum gap size is dependent of the initial energy only and thus independent of the initial velocity.

A. Capture basin based gap size

In this section is discussed how large the gap size is, if the model selects the $N = 1$ boundaries of the capture basin for any initial condition. The gap size between two subsequent steps depends on the initial conditions of the SLIP-model and the angle of attack of the steps.

In order to maximize the gap between to subsequent steps, it can be understand it is beneficial to have the 1^{st} step location as far behind the point mass as possible and the 2^{nd} step location as far beyond the point mass as possible. The formula to determine the step location, equation (16) and Fig. (3), show the influence of the forward velocity of the model. Therefore, in order to maximize the gap size, the difference in forward velocity of two subsequent steps should be as big as possible.

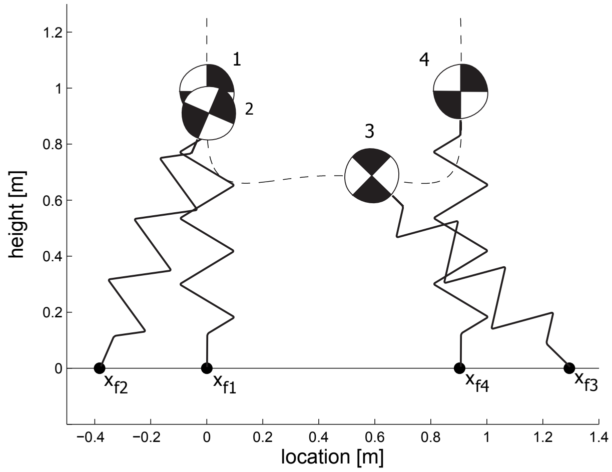

Fig. 6. 2-step strategy behavior with a preceding and subsequent step. The SLIP-model hops on one spot and touches down at (1). The model subsequently puts its foot as far backwards as possible at the boundary of the capture basin and touches down at (2). The next step location is obtained by putting the foot as far forwards as possible (3). The end position obtained is where the model touches down at (4). With this strategy, the model is only able to prevent falling down by selecting a step location for the preceding step (1) and following step 4) within the outer steps, (2) and (3), thereby reducing the gap size.

This method is used if the model selects the boundaries of the capture basin.

The model can put its leg behind the point mass by selecting the angle of attack such that $\alpha_0 > \frac{\pi}{2}$ in the first step, by selecting a state from the capture basin which is on the boundary of the 1-step region. The obtained gap size is maximal if the forward velocity is 0 m/s at start, as with an initial forward velocity larger than zero, the difference in gap size would be smaller. This strategy causes the SLIP-model to put its leg backwards as far as possible, causing the model shoot forward, gaining a high forward velocity. Subsequently, the model can put its leg as far forwards as possible to maximize the step size, by selecting another state from the capture basin which is on the boundary of the 1-step region.

However, in order to prevent falling down, the preceding and consecutive step locations would lie in between the step locations of the leap with this strategy. This situation can be seen in Fig. 6. As the obtained gap size with this strategy is reduced, a different strategy is necessary which avoids the previous stated problem.

B. 4-step Strategy

In Section IV-A is shown that a 2-step strategy limits the gap size, as the model needs to step within the obtained gap size range to prevent falling down. In this section a 4-step strategy is proposed, which is able to maximize gap size, without the necessity of stepping in between the step locations of the leap.

The 4-step strategy consists out of three distinct phases: The first phase is an adaptive step$^{(1)}$, in which the angle of attack can be chosen such that the upcoming apex has the optimal state conditions for the beginning of the leap. The second phase is the leap and consists out of step$^{(2)}$ and step$^{(3)}$. The distance between the 2^{nd} and 3^{rd} step location is the gap size to be maximized. The third phase is another adaptive step$^{(4)}$, in which the angle of attack is chosen such that a desired end state is reached. Fig. 7 shows the three phases and its associated steps and step locations, showing the trajectory of the model and its return to its initial condition.

In order to determine the largest gap size possible, an optimization is used to determine the step locations needed to obtain the maximum gap size. The optimization is implemented using the function `fmincon` in MATLAB. The objective to maximize is the gap size, denoted with $f(gap)$:

$$\begin{aligned} \max_{gap} f(gap) &= x_{end} - x_{start} \\ x_{start} &= \max[x_{f1}\ x_{f2}] \\ x_{end} &= \min[x_{f3}\ x_{f4}\ x_{CoM}{}^{(4)}] \end{aligned} \quad , \qquad (17)$$

in which x_{f1}, x_{f2}, x_{f3} and x_{f4} are the step locations of the associated steps and $x_{CoM}{}^{(4)}$ is the location of the point mass at x_{a4}. The location of the point mass is incorporated in the gap size optimization, as there is a possibility that the location of 3^{rd} and 4^{th} step location is beyond the location of $x_{CoM}{}^{(4)}$. In such a situation, a subsequent step could be necessary in order to prevent falling down, at a location before the 3^{rd} and 4^{th} step location. Then, falling down at $x_{CoM}{}^{(4)}$ can be prevented by setting the angle of attack to $\frac{\pi}{2}$ radians. The gap size is calculated between the first pair of steps and the second pair of steps. This forces the leap physically to be between the first pair of steps and the second pair of steps, but allows the optimization to select the order of steps in any way if desired.

The optimization is constrained by g and h, which are the inequality and equality constraints respectively:

$$\begin{aligned} g(gap) &= \alpha_i - \pi \quad \leq \quad 0 \quad \text{for} \quad i = 1\ldots4 \\ &= -\dot{x}_{a4} \quad \leq \quad 0 \\ h(gap) &= |q_4 - q_0| \quad = \quad 0 \end{aligned} \quad , \qquad (18)$$

in which α_1, α_2, α_3 and α_4 are the allowable angles of attack for the four subsequent steps, $\dot{x}_{a4}$ is the velocity at apex$^{(4)}$ and q_0 and q_4 are the begin state and end state of the optimization respectively. If the objective is to return to limit cycle running, than q_4 should be equal to q_0. However, if the desired end state is hopping with zero forward velocity, than the end state should be $q_4 = [E\ 0]^T$. The optimization is described in more detail in Appendix B.

V. Results

The results for the optimization of the 4-step strategy presented in Section IV-B are discussed in this section. We show that the maximum gap size is almost independent of the initial velocity and that the gap size mostly depends on the initial energy level. Subsequently is presented that the 1^{st} and 2^{nd} step location should coincide in order to maximize the gap size. In order to return to the initial state of the model, the 3^{rd} and 4^{th} step location should coincide as well. The gap size

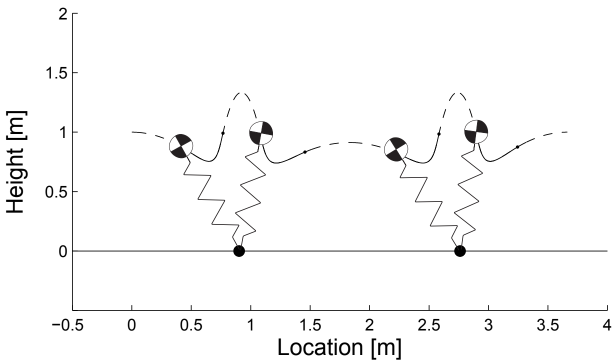

(a) Trajectory SLIP - initial condition return

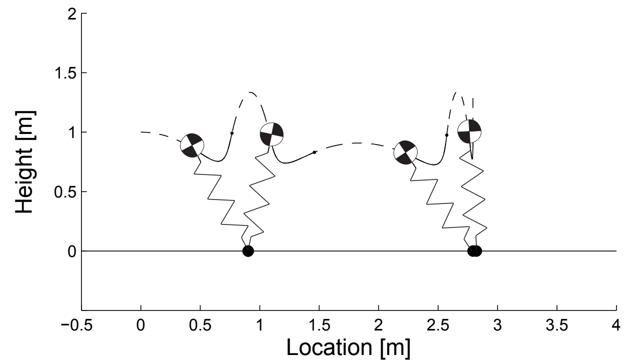

(b) Trajectory SLIP - capture point

Fig. 7. 4-step strategy behavior. The first touchdown of the SLIP-model is at (1), the model locates its foot at such an angle that the second touchdown is possible at the same step location (2). The model leaps to the third touchdown (3) and the angle of attack at the last touchdown (4) can be chosen such that model ends in a desired condition. Fig. 7(a) shows return to initial conditions, whereas Fig. 7(b) shows ending in hopping with zero forward velocity.

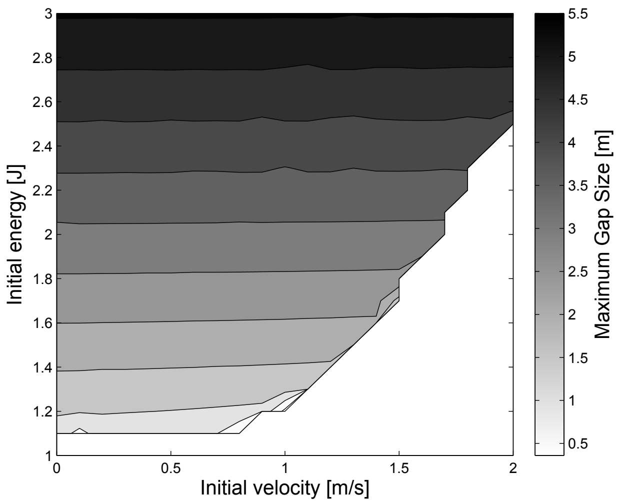

Fig. 8. The maximum gap size for a range of initial conditions. At lower energy levels, no solution is found for higher initial velocities. The initial height is to low to successful make four steps. The figure shows that the maximum gap size is almost independent of the initial velocity.

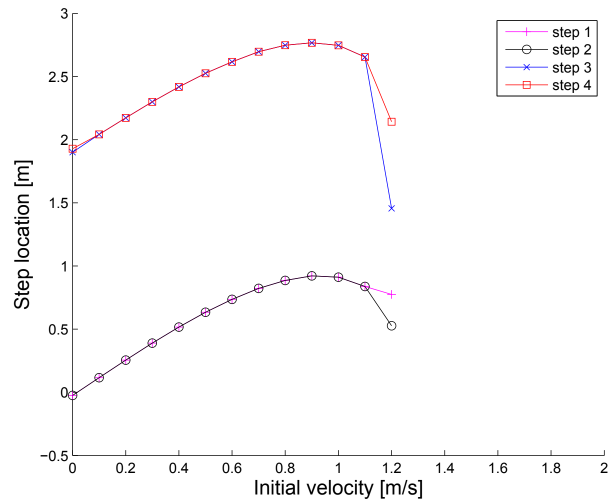

Fig. 9. Step locations for a constant energy level and a range of initial velocities. The optimization is set such that the model returns to its initial conditions. The figure shows that the 1^{st} and 2^{nd} step location and the 3^{rd} and 4^{th} step location coincide. Furthermore, the figure shows that there is almost no influence of the initial velocity to the gap size, barring the boundary conditions.

is increased even further if the 4^{th} step location is positioned at the capture point. This causes the model to hop with zero velocity at the end of the step sequence. However, the gap size increases only slightly in relation to the gap size obtained for initial state return.

Fig. 8 shows the maximum gap size for the range of initial velocities $\dot{x}_0 = [0 - 2]$ m/s and energy levels $E = [1.1 - 3]$ J. The gap size is calculated with the constraint that the model should return to its initial condition after four steps. The figure shows that the maximum gap size is mostly dependent of the initial energy level, the initial velocity has almost no influence to the gap size. The lower right hand side of the figure shows no solutions for the optimization, as at lower energy levels with higher initial velocities, the initial height is to low for the model to successful make four steps.

Fig. 9 shows the four step locations for the range of initial velocities $\dot{x}_0 = [0 - 2]$ m/s at an energy level of $E = 1.35$ J. The gap size is calculated with the constraint that the model should return to its initial conditions. The figure shows that the 1^{st} and 2^{nd} step location and the 3^{rd} and 4^{th} step location coincide. Furthermore, the maximum gap size is almost independent of the initial velocity, barring the outer solutions. At initial velocities higher than 1.2 m/s no solutions are found, as the initial height is to low for a successful sequence of four steps. The initial velocity of $\dot{x}_0 = 1.2$ m/s results in a successful sequence of steps. However, the gap size is significant reduced and the step locations do not coincide.

Fig. 10 shows the four step locations for a constant initial velocity of $\dot{x}_0 = 0.8$ m/s, at an energy range of $E_s =$

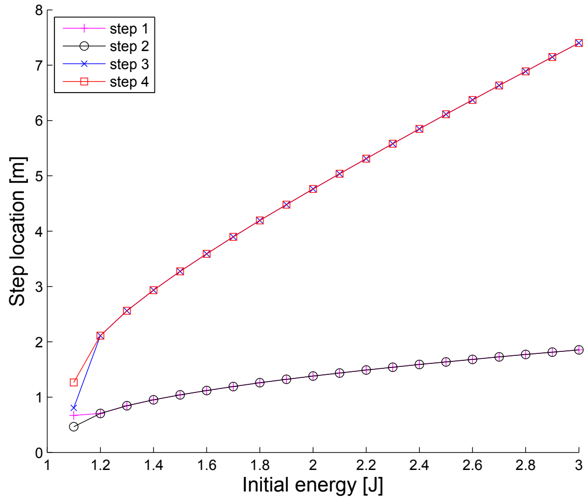

Fig. 10. Step locations for a constant initial velocity and a range of energy levels. The optimization is set such that the model returns to its initial conditions. The figure shows that the 1^{st} and 2^{nd} step location and the 3^{rd} and 4^{th} step location coincide. Furthermore, the figure shows that the maximum gap size increases with the energy level of the system.

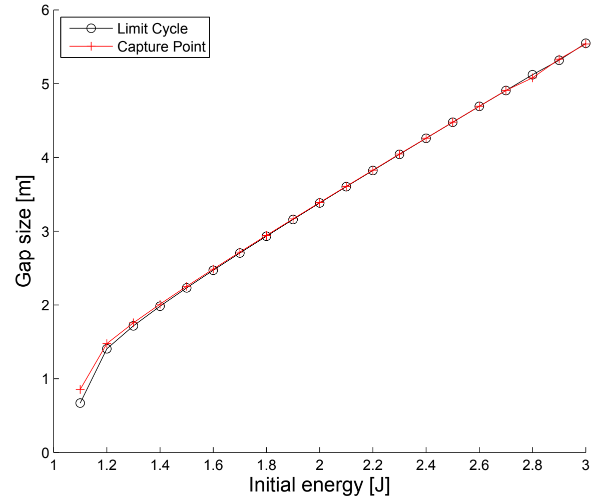

Fig. 11. Maximum gap size for a simulation ending in limit cycle running and a simulation ending in its capture point end state. The figure shows that the maximum gap size difference obtained for capture point end state and limit cycle return is small.

$[1.1 \; - \; 3]\; J$. The gap size is calculated with the constraint that the model should return to its initial conditions. The figure shows that the 1^{st} and 2^{nd} step location and the 3^{rd} and 4^{th} step location coincide and the gap size increases with the energy level of the system. At an energy level of $E = 1.1\; J$ it can be seen that a success sequence is possible, yet the low initial height reduces the gap size.

If the model does not have to end in a limit cycle condition, than the 3^{rd} and 4^{th} step location might be chosen differently in order to obtain a bigger gap size. Fig. 11 shows the maximum gap size calculated for two different end constraints. The first constraint demands the model to return to its initial condition, whereas the second constraint demands the model to step on its capture point. The gap size is calculated for an energy range of $E_s = [1.1 \; - \; 3]\; J$ and with an initial velocity of $0.8\; m/s$. The figure shows that the obtained result differences are small, and that returning to the capture point results in a slightly larger gap size.

VI. Discussion

The results achieved with the optimization are not intuitive for every situation. This section explains the behavior of the optimization and discusses the results in detail. Section VI-A discusses the coincident step locations obtained for the 4-step strategy optimization. Section VI-B discusses the influence of the initial velocity to the maximum gap size. The influence of the damper and the push-off is discussed in Section VI-C. Section VI-D discusses the behavior of the optimization compared with the behavior of humans and discusses whether the SLIP model is a good model for such an optimization.

A. Explanation Of Coincident Step Locations

The step strategy to obtain the maximum gap size per energy level shows a sequence of step locations which is shown in Fig. 9 and 10. The 1^{st} and 2^{nd} step locations and the 3^{rd} and 4^{th} step locations coincide if the model returns to its initial condition. This section explains the coincident step locations.

In order to explain whether coincident step locations lead to the maximum gap size, an extra optimization is induced. The distance of the point mass at x_{a2}, which is halfway of the leap, is calculated for different locations of the 1^{st} and 2^{nd} step location. The 1^{st} step location is determined for every angle of attack in the range $[0 \; - \; \pi]$ radians. By setting a desired state at x_{a2}, the 2^{nd} step location can be determined with the use of an optimization.

However, only one state variable can be set as a desired value, as there is only one variable to tune, which is the angle of attack of step$^{(2)}$. Therefore, the desired value at x_{a2} is set to the velocity $\dot{x}_{des}$ equally to the velocity at x_{a2} obtained by the optimization in Section IV-B.

The maximum gap size occurs where the largest of the two step locations subtracted from the position of the point mass at x_{a2} is maximal. The optimization is implemented using the function `fmincon` in MATLAB and is started with an energy level of $E = 1.35\; J$, initial velocity of $\dot{x}_0 = 0.8\; m/s$ and $\dot{x}_{des} = 0.94\; m/s$. The objective to maximize is half of the gap size, denoted with $f(^1\!/\!_2\; gap)$:

$$\begin{aligned} \max_{^1\!/\!_2\; gap} f(^1\!/\!_2\; gap) &= x_{end} - x_{start} \\ x_{start} &= \max[x_{f1}\; x_{f2}] \\ x_{end} &= {x_{CoM}}^{(2)} \end{aligned} \quad , \qquad (19)$$

in which x_{f1} and x_{f2} are the step locations of the associated steps. ${x_{CoM}}^{(2)}$ is the location of the point mass at x_{a2}, which is the highest point of the flight phase during the leap.

The optimization is constrained by g and h, which are the inequality and equality constraints respectively:

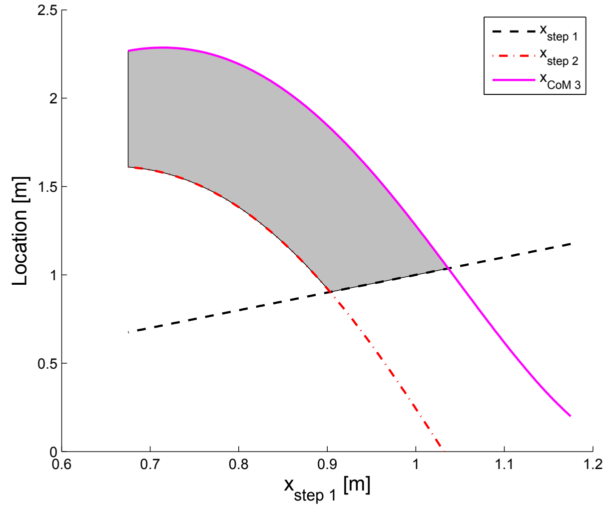

Fig. 12. Coincident step locations result in the largest gap size. The step location of step$^{(1)}$ is represented by the dashed line, whereas the dash-dotted line represents the step location of step$^{(2)}$. The solid line represents the location of the point mass at apex at the end of step$^{(2)}$. The gray area represents half of the max gap size and this is determined by subtracting the largest of the step locations from the point mass location of at the end of step$^{(2)}$. It can be seen that the gap size is maximal when the foot steps coincide.

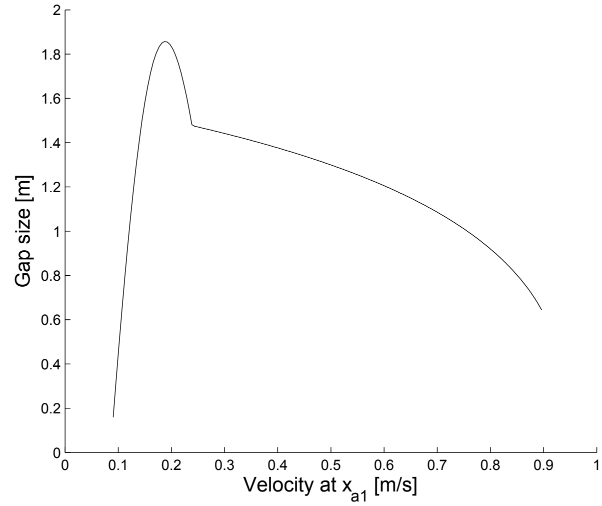

Fig. 13. The influence of the velocity at x_{a1} to the maximum gap size. The gap size is calculated for several velocities at x_{a1} prior step$^{(2)}$. The optimization is constrained such that the 1^{st} and 2^{nd} step location coincide. The figure shows that the gap size is maximal for a low velocity at x_{a1}.

$$\begin{array}{rclcl} g\left(1/2\ gap\right) & = & \alpha_2\ - \pi & \leq & 0 \\ h\left(1/2\ gap\right) & = & \left|\dot{x}_{q2} - \dot{x}_{des}\right| & = & 0 \end{array} , \tag{20}$$

in which α_2 is the allowable angle of attack for the second step. The velocities $\dot{x}_{q2}$ and $\dot{x}_{des}$ are the velocity at x_{a2} and the desired velocity at x_{a2} respectively.

Fig. 12 shows the 1^{st} and 2^{nd} step locations and the location of the point mass at x_{a2} plotted against the 1^{st} step location. The gray area represents half of the maximum gap size determined with the optimization by subtracting the largest of the step locations from the point mass location at x_{a2}. The figure shows that distance of the step locations to the location of x_{a2} is maximal if the step locations coincide. We believe that coincident step locations lead to the largest gap size possible, as the gap size reduces if there is an offset between the 1^{st} and 2^{nd} step location, independently of the order of the steps.

B. Influence Of Initial Velocity

The maximum gap size is, barring the boundaries, almost independent of the initial velocity and mostly dependent of the energy level of the system as can be seen in Fig. 8 and 9. This section discusses the influence of the initial velocity to the gap size.

In Section VI-A it is shown that the step locations have to be coincident in order to maximize the gap size. In order to achieve this, the 4-step optimization has to adjust any initial velocity such that the forward velocity at x_{a1} still allows the 2^{nd} step location to coincide with the 1^{st} step location.

In order to explain why the initial velocity has no influence to the maximum gap size, an extra optimization is induced. The distance of the point mass at x_{a2}, which is halfway of the leap, is calculated for different locations of coincident step locations. The 1^{st} and 2^{nd} step location are determined for every angle of attack in the range $[0\ -\ \pi]$ radians. The velocity at x_{a1} is known due to the constraint of coincident step locations. The maximum gap size can now be determined for the optimal velocity at x_{a1}.

The optimization is implemented using the function `fmincon` in MATLAB and is started with an energy level of $E = 1.35\ J$ and an initial velocity of $\dot{x}_0 = 0.8\ m/s$. The objective to maximize is half of the gap size, dependent of the velocity at apex$^{(1)}$, which is denoted as $f(\dot{x}_{a1})$:

$$\begin{array}{rcl} \max\limits_{\dot{x}_{a1}} f(\dot{x}_{a1}) & = & x_{end} - x_{start} \\ x_{start} & = & \max[x_{f1}\ x_{f2}] \\ x_{end} & = & {x_{CoM}}^{(2)} \end{array} , \tag{21}$$

in which x_{f1} and x_{f2} are the step locations of the associated steps. ${x_{CoM}}^{(2)}$ is the location of the point mass at x_{a2}, which is the highest point of the flight phase during the leap.

The optimization is constrained by g and h, which are the inequality and equality constraints respectively:

$$\begin{array}{rclcl} g(\dot{x}_{a1}) & = & \alpha_2\ - \pi & \leq & 0 \\ h(\dot{x}_{a1}) & = & x_{f2} - x_{f1} & = & 0 \end{array} , \tag{22}$$

in which α_2 is the allowable angle of attack for the second step and x_{f1} and x_{f2} are the 1^{st} and 2^{nd} step location respectively.

Fig. 13 shows the maximum gap size for a range of velocities at the x_{a1}. The figure shows that the gap size is maximal if the velocity at x_{a1} is $0.19\ m/s$, which is lower than the initial velocity. Furthermore, it can be seen that the gap size reduces if the velocity at x_{a1} is increased or further reduced. Hence it can be concluded that in order to maximize the gap size and to let the step locations coincide, the initial velocity

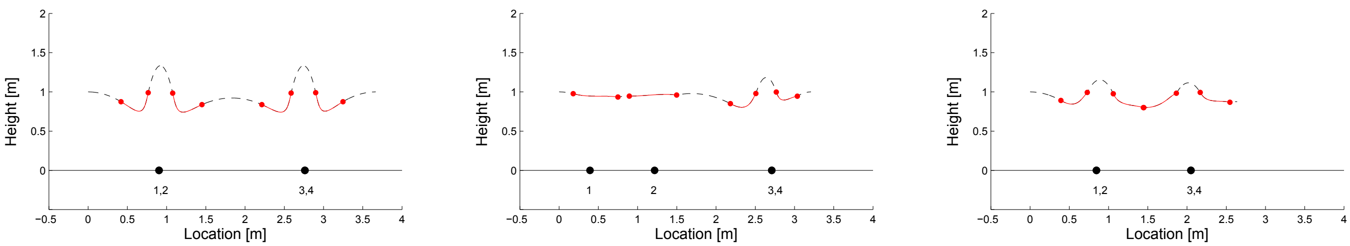

(a) Optimal trajectory SLIP (b) Optimal trajectory DSLIP (c) DSLIP trajectory with coincident steps

Fig. 14. Trajectory and gap size comparison for SLIP and DSLIP models. The stance phases during the steps are indicated with a solid line, in which the dots represent the touchdown and lift-off moments and the numbers indicate the step locations. All optimizations were started with energy level $E = 1.35\ J$ and initial velocity $\dot{x}_0 = 0.8\ m/s$. The trajectory for the SLIP-model in Fig. 14(a) shows coincident step locations, whereas the DSLIP-model in Fig. 14(b) only shows coincident step locations at the 3^{rd} and 4^{th} step. The gap size obtained for the SLIP-model is 1.86 m, whereas the gap for the DSLIP-model (14(b)) is 1.49 m. In Fig. 14(c), the DSLIP-model is constrained to have coincident step locations. The gap size obtained with this constraint is 1.20 m. Hence coincident step locations do not lead to the maximum gap size for the DSLIP-model.

has to be adjusted to a velocity at x_{a1} which still enables to let the 1^{st} and 2^{nd} step location coincide. We believe the reason that the initial velocity has a very small influence to the gap size, is caused by the gap size optimization. The optimization wants the step locations to coincide, which is only possible for a low velocity at x_{a1}. Therefore α_1 is chosen such that the velocity at x_{a1} is optimal for coincident step locations. The small influence of the initial velocity can be explained, as with a higher initial velocity, the initial height is reduced. A lower initial height reduces the possible step locations, thereby reducing the gap size.

C. Influence Of Damper And Push-off

In Section III is shown that the behavior of the SLIP and the DSLIP-model is similar if the capture point has to be calculated. Therefore the SLIP-model was used to determine the optimal step strategy in order to obtain the maximum gap size possible. This section compares the results found with the SLIP-model to an optimization implemented with the DSLIP-model in order to investigate whether damping and push-off have significant influence to the behavior and step sequence.

In order to compare the DSLIP-model to the SLIP-model, the optimization discussed in Section IV-B is implemented with the DSLIP-model. The energy level per step might vary due to the damping and the push-off. However, only one state variable can be set as a desired value, as there is only one variable to tune, which is the angle of attack of step. Therefore, the desired end value of the step sequence is set to be equal to the initial height of the system.

The optimization is implemented in the same manner as the 4-step optimization described in Section IV-B. The damping constant is 4.6 Ns/m and the push-off energy is $E_{push} = 0.1\ J$, these values are held constant for the sequence of steps. The optimization is constrained by g and h, which are the inequality and equality constraints respectively:

$$\begin{aligned} g(gap) &= \alpha_i - \pi &\leq 0 \quad \text{for} \quad i = 1 \ldots 4 \\ &= -\dot{x}_{a4} &\leq 0 \\ h(gap) &= |y_4 - y_0| &= 0 \end{aligned} \quad , \qquad (23)$$

in which α_1, α_2, α_3 and α_4 are the allowable angles of attack for the four subsequent steps, $\dot{x}_{a4}$ is the velocity at apex$^{(4)}$ and y_0 and y_4 are the initial height and end height of the optimization respectively.

Fig. 14(a) shows trajectory and step locations of the SLIP-model, whereas Fig. 14(b) shows trajectory and step locations of the DSLIP-model. The maximum gap size obtained for the SLIP-model is 1.86 m with the given initial conditions, whereas the maximum gap size obtained for the DSLIP-model is 1.49 m, which is a reduction of 20%. The SLIP-model optimization shows for the 1^{st} and 2^{nd} step and the 3^{rd} and 4^{th} step coincident step locations, whereas the optimization results for the DSLIP-model only show coincident step locations for 3^{rd} and 4^{th} step.

The result obtained for the optimization with the DSLIP-model does not show coincident step locations for the 1^{st} and 2^{nd} step. For the SLIP-model was found that coincident step locations is optimal to maximize the gap size. In order to investigate whether the found step sequence with the DSLIP-model optimization is the optimal sequence, a new optimization is induced. The gap size is optimized for the DSLIP-model, with the additional constraint that the 1^{st} and 2^{nd} step location and the 3^{rd} and 4^{th} step location should coincide.

The optimization is implemented in the same manner as the 4-step optimization described in Section IV-B. The optimization is constrained by g and h, which are the inequality and equality constraints respectively:

$$\begin{aligned} g(gap) &= \alpha_i - \pi &\leq 0 \quad \text{for} \quad i = 1 \ldots 4 \\ &= -\dot{x}_{a4} &\leq 0 \\ h(gap) &= x_{f2} - x_{f1} &= 0 \\ &= x_{f4} - x_{f3} &= 0 \end{aligned} \quad , \qquad (24)$$

in which α_1, α_2, α_3 and α_4 are the allowable angles of attack for the four subsequent steps, $\dot{x}_{a4}$ is the velocity at apex$^{(4)}$ and x_{f1}, x_{f2}, x_{f3} and x_{f4} are the step locations of the associated steps.

Fig. 14(c) shows the trajectory and step locations of the DSLIP-model with coincident step locations. The maximum gap size obtained for the DSLIP-model is 1.20 *m* with the given initial conditions, which is 19% shorter than the optimization for the DSLIP-model without the coincident step location constraint and 35% shorter than the SLIP-model.

In Section VI-B is shown that in order to obtain coincident step locations, the forward velocity at apex$^{(2)}$ should be such that the 2^{nd} step location still can coincide with the 1^{st} step location. However, due to the coincident step location constraint and the reduced energy at lift-off, the gained forward velocity at lift-off in Fig. 14(c) is lower than the lift-off velocity obtained for the optimization in Fig. 14(b). This results in a smaller gap size for the DSLIP-model. Hence for the DSLIP-model, coincident step locations do not lead to the maximum gap size possible.

The results obtained for the DSLIP-model optimizations show different trajectories and smaller gap sizes than obtained for the SLIP-model, thus it can be concluded that the system energy is an important state in obstacle overstepping. All of the system energy remains available at lift-off with the SLIP-model, hence the model is able to position the leg at all angles in the subsequent step. The reduced energy at lift-off has evidently influence to the behavior of the model and the gap size. For the DSLIP-model can be concluded that coincident step locations do not lead to the optimal step strategy to maximize the gap size.

D. Relation To Human Behavior

This simulation study focuses completely on robotic obstacle overstepping, in which the SLIP-model is used. Research has shown that running gaits calculated with the SLIP-model are similar to human running gaits, hence the question rises what humans would do.

Step location preference has been studied [13–16] and it is shown that humans start to adjust their gait in the last two steps prior overstepping an obstacle [17]. However, an exact step planning strategy is not known yet and there is no mention of coincident step locations. This suggests that although the SLIP-model gives similar results to human running gaits, the model is not used for activities other than normal running. The DSLIP-model does provide different results than the SLIP-model, although the applied damping and push-off method might be chosen differently. The simulations do show that the behavior of the SLIP and DSLIP-model is in agreement with the results found by Mohagheghi et al. [17], which is that the robot needs two steps to adjust prior overstepping an obstacle.

The SLIP-model is a simplified model for human and robotic running and gives similar results for normal running. However, in a task such as given, what would be the influence of ankles and knees towards the optimal step locations? When the SLIP-model leaps the gap, the velocity to height ratio is relatively high. Due to the massless leg of the model, it is able to position the leg such as it desires. However, humans do not have massless legs, they have knees and ankles and they have to be able to move their legs from one step location to the other. These influences could be investigated and simulated with the SLIP-model by adding mass to the legs, introduce a minimal step time between two subsequent steps, or adding a finite size foot.

VII. Conclusion

In this paper, the goal was to determine step locations for running robots in order to overstep the largest possible gap. This goal is investigated by the means of a simulation study and it can be concluded that the optimal step locations can be determined for running robots in order to obtain the largest gap possible. From the results we conclude that:

- the method to determine the capture points and capture regions for walking robots can not be used for running robots,
- for the SLIP-model, a 4-step strategy is minimally required to maximize the gap size. The strategy consists out of three phases, which are an adaptive step, the leap and another adaptive step,
- for the SLIP-model, the gap size is almost independent of the initial velocity and mostly depends of the initial energy level,
- for the SLIP-model, the first and second step location should coincide to maximize the gap size,
- for the SLIP-model, the gap size is maximal if the model ends with zero velocity at the end of the fourth step,
- for the DSLIP-model, the system energy and energy prove to be important factors, as the gap size is reduced significantly and the step strategy does not feature coincident step locations at the first and second step location.

VIII. Recommendations

Although successful obstacle overstepping is achieved, other methods to select the step locations can be used. Robots are not humans, therefore it is recommended to explore alternative methods. Interesting would be to minimize the energy used to overstep an obstacle, or to add extra constraints like leg or feet mass and therefore inertia. The SLIP-model only features one leg and the obtained trajectories might be different with two legs. The damping constant in the DSLIP-model is set to a fixed value, which is determined on the energy losses reported by Raibert et al. [32], although a damping constant determined for the robot Phides could be used. Furthermore, the dashpot only functions if the velocity of the leg is negative. For a more realistic behavior the damping could work in both directions. The push-off is set to be added instantaneous at lift-off with a fixed amount of energy, whereas different behavior might be obtained if the amount of energy added would vary and the energy could be added gradually. Furthermore, the addition of leg mass could make the model behavior more realistic. Experiments on the robot Phides can serve as a measure for which the SLIP and DSLIP-model are valid for this specific robot and this specific task.

Appendix A
Determinating the Capture Basin

The capture basin shows per initial condition the number of steps minimal needed to come to a standstill, in which 'standstill' means no forward movement; the model will remain hopping on the same location. The general idea of the capture basin is as follows. For every input state q_{in} is calculated what the end state q_{out} is. Comparing between the input and output states can tell the number of steps for which the model can come to a full stop, also called the number of steps for which the model is capturable.

The calculation of the capture basin is an iterative process, which is calculated per energy level. The lower boundary of the capture basin is at $E = 1\ J$, as this is the boundary at which the model can come to a standstill. For energy levels lower than 1 J, the model is not able to put its leg at an angle of $\frac{\pi}{2}$, as the height of the model is to low. The upper boundary is arbitrarily chosen at $E = 5\ J$. The total dimension of the capture basin is equal to the grid size of $\dot{x}_0 \times E$.

For N-step capturability, the value of the capture basin R is determined per initial velocity. For all successive calculated steps (no falling down), the minimum and maximum output velocities are stored. This process is repeated for a range of initial velocities $\dot{x}_0 = [-5, 5]\ m/s$. Subsequently, per successful step the minimum and maximum input velocity $\dot{x}_{in}$ are stored. The 0-step capture basin is determined by any combination for which the input velocity 0 m/s is. With deduction can be determined if the system is 1-step capturable or higher. The value per element in R is given by:

$$R = N, \quad \text{if} \quad \begin{cases} \dot{x}_{max_{out}} & \geq & \dot{x}_{min_{in}} \\ \dot{x}_{min_{out}} & \leq & \dot{x}_{max_{in}} \end{cases}, \tag{25}$$

in which $\dot{x}_{min_{in}}$, $\dot{x}_{max_{in}}$, $\dot{x}_{min_{out}}$ and $\dot{x}_{max_{out}}$ are the minimal and maximal input and output velocity respectively.

If the output velocities of the step lie within the boundaries given in equation (25), then value the of the element in R is updated to $N = 1$. Subsequently, the next element of R is calculated for its associated input velocity. If the system is not 1-step capturable, the process is repeated with different initial conditions. If the system is now capturable, the value of R is updated to $N = 2$. In pseudo code, this process looks as follows:

Select speed ranges:
    $q_0 = [y_0\ \dot{x}_0]$ & $\alpha_0 = [0 - \pi]$
        $\rightarrow$ simulate step
            $\rightarrow$ select $\dot{x}_{min_{out}}$ & $\dot{x}_{max_{out}}$ per $\dot{x}_{in}$
                $\rightarrow$ store all $\dot{x}_{min_{out}}$ & $\dot{x}_{max_{out}}$ values
Determining Capture Range R:
    $\rightarrow$ start at $n = 0$
        $\rightarrow$ select $\dot{x}_{min_{in}}$ & $\dot{x}_{max_{in}}$ from input $\dot{x}_0$
        $\rightarrow$ $R\left(\dot{x}_{max_{out}} \geq \dot{x}_{min_{in}} \& \ \dot{x}_{min_{out}} \leq \dot{x}_{max_{in}}\right) = n$

Appendix B
Step Location Optimization

The 4-step strategy consists out of three distinct phases: The first phase is an adaptive step$^{(1)}$, in which the angle of attack can be chosen such that the upcoming apex has the optimal state conditions for the beginning of the leap. The second phase is the leap and consists out of step$^{(2)}$ and step$^{(3)}$. The distance between the 2^{nd} and 3^{rd} step location is the gap size to be maximized. The third phase is another adaptive step$^{(4)}$, in which the angle of attack is chosen such that a desired end state is reached. In order to determine the largest gap size possible, an optimization is used to determine the step locations needed to obtain the maximum gap size. This appendix describes in detail the optimization process.

The objective of the optimization is to maximize the gap size, which is the distance between the 2^{nd} and 3^{rd} step location. In order to maximize the gap size, it is necessary to calculate the end conditions of four steps and their associated step locations. The initial condition is denoted with q_0, which is the vector containing the initial energy level and velocity:

$$q_0 = \begin{bmatrix} E_0 \\ \dot{x}_0 \end{bmatrix} \tag{26}$$

As the model is described by its energy level and velocity, the initial height is determined by:

$$y_0 = \frac{E_0 - \frac{1}{2}m\dot{x}_0^2}{mg} \tag{27}$$

An angle of attack can be set to make a step, the end state after making a step is denoted with q_1, which is also the input state for the subsequent step. If the model makes four steps, the states are denoted q_0 to q_4 and the associated angles of attack α_1 to α_4. The relative step locations can be calculated with:

$$x_{f(i)} \quad = \quad \dot{x}_i\sqrt{2y_i - \sin\alpha_i} + l_0\cos\alpha_i \quad \text{for} \quad i = 0\ldots4\ , \tag{28}$$

in which x_{fi}, $\dot{x}_i$, y_i and α_i are the step location, velocity, height and the angle of attack of the model respectively. In order to determine the absolute step locations of the four subsequent steps, the location of the point mass at the end of each step has to be added to the relative step location:

$$\begin{aligned} x_{f1} &= x_{f1} \\ x_{f2} &= x_{f2} + x_{CoM}{}^{(1)} \\ x_{f3} &= x_{f3} + x_{CoM}{}^{(1)} + x_{CoM}{}^{(2)} \\ x_{f4} &= x_{f4} + x_{CoM}{}^{(1)} + x_{CoM}{}^{(2)} + x_{CoM}{}^{(3)} \end{aligned} \tag{29}$$

in which $x_{CoM}{}^{(1)}$, $x_{CoM}{}^{(2)}$ and $x_{CoM}{}^{(3)}$ are the locations of the center of mass after the preceding step.

The optimization is implemented using the function `fmincon` in MATLAB. The objective to maximize is the gap size, denoted with $f(gap)$:

$$\begin{array}{rcl} \max_x f(gap) & = & x_{end} - x_{start} \\ x_{start} & = & \max[x_{f1}\ x_{f2}] \\ x_{end} & = & \min[x_{f3}\ x_{f4}\ x_{CoM}{}^{(4)}] \end{array} , \quad (30)$$

in which x_{f1}, x_{f2}, x_{f3} and x_{f4} are the step locations of the associated steps and $x_{CoM}{}^{(4)}$ is the location of the point mass after the 4^{th} step. The location of the point mass is incorporated in the gap size optimization, as there is a possibility that the location of 3^{rd} and 4^{th} step location is beyond the location of $x_{CoM}{}^{(4)}$. In such a situation, a subsequent step could be necessary in order to prevent falling down, at a location before the 3^{rd} and 4^{th} step location. Then, falling down at $x_{CoM}{}^{(4)}$ can be prevented by setting the angle of attack to $\frac{\pi}{2}$ radians. The gap size is calculated between the first pair of steps and the second pair of steps. This forces the leap physically to be between the first pair of steps and the second pair of steps, but allows the optimization to select the order of steps in any way if desired.

In order to start the optimization successfully, the input angles should have a valid solution. The first angle is set to the capture point, whereas the subsequent angles are set to let the model hop on the same spot:

$$\alpha_i = \left[\begin{array}{cccc} \alpha_{cp} & \frac{\pi}{2} & \frac{\pi}{2} & \frac{\pi}{2} \end{array} \right], \quad (31)$$

in which α_{cp} is the angle of attack, which is chosen such that the input state $q_0 = [E_0\ \dot{x}_0]^T$ is transformed into the end state $q_1 = [E_1\ 0]^T$. The angle α_{cp} to obtain this desired end state is determined by the means of a separate optimization implemented in MATLAB using the function `fminsearch`.

The optimization is constrained by g and h, which are the inequality and equality constraints respectively:

$$\begin{array}{rclcll} g(gap) & = & \alpha_i - \pi & \leq & 0 & \text{for} \quad i = 1 \ldots 4 \\ & = & -\dot{x}_{a4} & \leq & 0 & \\ h(gap) & = & |q_4 - q_0| & = & 0 & \end{array} , \quad (32)$$

in which α_1, α_2, α_3 and α_4 are the allowable angles of attack for the four subsequent steps, $\dot{x}_{a4}$ is the velocity at x_{a4} and q_0 and q_4 are the begin state and end state of the optimization respectively.

The inequality constraints are set such that the model puts its leg in allowable positions during the sequence of four steps and to ensure that the horizontal velocity at the end of the sequence is zero or positive. The equality constraint is set such that the model ends in a desired end state. If the desired end state is equal to the initial state, than q_4 is equal to q_0. However, if the desired end state is hopping with zero forward velocity, than the end state should be $q_4 = [E\ 0]^T$.

The optimization outputs the four angles of attack necessary to obtain the maximum gap size, and the obtained gap size. This process is initiated for energy levels in the range of $E = [1.1\ -\ 3]\ J$ and initial velocities of $\dot{x}_0 = [0\ -\ 2]\ m/s$ with increments of 0.1 per step.

References

[1] R. Alexander. Three uses for springs in legged locomotion. *The International Journal of Robotics Research*, 9(2):53–61, 1990.

[2] B. Brown and G. Zeglin. The bow leg hopping robot. In *Robotics and Automation, 1998. Proceedings. 1998 IEEE International Conference on*, volume 1, pages 781–786. IEEE, 1998.

[3] M. Ahmadi and M. Buehler. The arl monopod ii running robot: Control and energetics. In *Robotics and Automation, 1999. Proceedings. 1999 IEEE International Conference on*, volume 3, pages 1689–1694. IEEE, 1999.

[4] M.H. Raibert, H.B. Brown Jr, and M. Chepponis. Experiments in balance with a 3d one-legged hopping machine. *The International Journal of Robotics Research*, 3(2):75–92, 1984.

[5] M. Hirose and K. Ogawa. Honda humanoid robots development. *Philosophical Transactions of the Royal Society A: Mathematical, Physical and Engineering Sciences*, 365(1850):11–19, 2007.

[6] R. Niiyama, S. Nishikawa, and Y. Kuniyoshi. Athlete robot with applied human muscle activation patterns for bipedal running. In *IEEE-RAS International Conference on Humanoid Robots (Humanoids 2010)*, pages 498–503, 2010.

[7] JW Grizzle, J. Hurst, B. Morris, H.W. Park, and K. Sreenath. Mabel, a new robotic bipedal walker and runner. In *American Control Conference, 2009. ACC'09.*, pages 2030–2036. IEEE, 2009.

[8] D. Papadopoulos and M. Buehler. Stable running in a quadruped robot with compliant legs. In *Robotics and Automation, 2000. Proceedings. ICRA'00. IEEE International Conference on*, volume 1, pages 444–449. IEEE, 2000.

[9] C. Semini, N.G. Tsagarakis, B. Vanderborght, Y. Yang, and D.G. Caldwell. Hyq-hydraulically actuated quadruped robot: Hopping leg prototype. In *Biomedical Robotics and Biomechatronics, 2008. BioRob 2008. 2nd IEEE RAS & EMBS International Conference on*, pages 593–599. IEEE, 2008.

[10] U. Saranli, M. Buehler, and D.E. Koditschek. Rhex: A simple and highly mobile hexapod robot. *The International Journal of Robotics Research*, 20(7):616–631, 2001.

[11] J.E. Clark, J.G. Cham, S.A. Bailey, E.M. Froehlich, P.K. Nahata, M.R. Cutkosky, and R.J. Full. Biomimetic design and fabrication of a hexapedal running robot. In *Robotics and Automation, 2001. Proceedings 2001 ICRA. IEEE International Conference on*, volume 4, pages 3643–3649. IEEE, 2001.

[12] R. Tajima, D. Honda, and K. Suga. Fast running experiments involving a humanoid robot. In *Robotics and Automation, 2009. ICRA'09. IEEE International Conference on*, pages 1571–1576. IEEE, 2009.

[13] A.E. Patla, C. Robinson, M. Samways, and C.J. Armstrong. Visual control of step length during overground locomotion: task-specific modulation of the locomotor

synergy. *Journal of Experimental Psychology: Human Perception and Performance*, 15(3):603–617, 1989.
[14] A.E. Patla, S.D. Prentice, S. Rietdyk, F. Allard, and C. Martin. What guides the selection of alternate foot placement during locomotion in humans. *Experimental Brain Research*, 128(4):441–450, 1999.
[15] V. Weerdesteyn, B. Nienhuis, B. Hampsink, and J. Duysens. Gait adjustments in response to an obstacle are faster than voluntary reactions. *Human movement science*, 23(3-4):351–363, 2004.
[16] V. Weerdesteyn, B. Nienhuis, T. Mulder, and J. Duysens. Older women strongly prefer stride lengthening to shortening in avoiding obstacles. *Experimental Brain Research*, 161(1):39–46, 2005.
[17] A. Mohagheghi, R. Moraes, and A.E. Patla. The effects of distant and on-line visual information on the control of approach phase and step over an obstacle during locomotion. *Experimental Brain Research*, 155(4):459–468, 2004.
[18] J. Chestnutt, J. Kuffner, K. Nishiwaki, and S. Kagami. Planning biped navigation strategies in complex environments. In *IEEE Int. Conf. Hum. Rob., Munich, Germany*, 2003.
[19] J. Chestnutt, M. Lau, G. Cheung, J. Kuffner, J. Hodgins, and T. Kanade. Footstep planning for the honda asimo humanoid. In *Robotics and Automation, 2005. ICRA 2005. Proceedings of the 2005 IEEE International Conference on*, pages 629–634. IEEE, 2005.
[20] J.K. Lee and S.M. Song. Path planning and gait of walking machine in an obstacle-strewn environment. *Journal of robotic systems*, 8(6):801–827, 1991.
[21] T.Y. Li, P.F. Chen, and P.Z. Huang. Motion planning for humanoid walking in a layered environment. In *Robotics and Automation, 2003. Proceedings. ICRA'03. IEEE International Conference on*, volume 3, pages 3421–3427. IEEE, 2003.
[22] J.J. Kuffner, S. Kagami, K. Nishiwaki, M. Inaba, and H. Inoue. Dynamically-stable motion planning for humanoid robots. *Autonomous Robots*, 12(1):105–118, 2002.
[23] Q. Huang, K. Yokoi, S. Kajita, K. Kaneko, H. Arai, N. Koyachi, and K. Tanie. Planning walking patterns for a biped robot. *Robotics and Automation, IEEE Transactions on*, 17(3):280–289, 2001.
[24] K. Harada, S. Kajita, K. Kaneko, and H. Hirukawa. An analytical method on real-time gait planning for a humanoid robot. In *Humanoid Robots, 2004 4th IEEE/RAS International Conference on*, volume 2, pages 640–655. IEEE, 2004.
[25] J.S. Gutmann, M. Fukuchi, and M. Fujita. A floor and obstacle height map for 3d navigation of a humanoid robot. In *Robotics and Automation, 2005. ICRA 2005. Proceedings of the 2005 IEEE International Conference on*, pages 1066–1071. IEEE, 2005.
[26] J.K. Hodgins and M.N. Raibert. Adjusting step length for rough terrain locomotion. *Robotics and Automation, IEEE Transactions on*, 7(3):289–298, 2002.
[27] E.R. Dunn and R.D. Howe. Foot placement and velocity control in smooth bipedal walking. In *Robotics and Automation, 1996. Proceedings., 1996 IEEE International Conference on*, volume 1, pages 578–583. IEEE, 2002.
[28] J. Pratt, J. Carff, S. Drakunov, and A. Goswami. Capture point: A step toward humanoid push recovery. In *Humanoid Robots, 2006 6th IEEE-RAS International Conference on*, pages 200–207. IEEE, 2006.
[29] R. Blickhan. The spring-mass model for running and hopping. *Journal of biomechanics*, 22(11-12):1217–1227, 1989.
[30] R. Blickhan and RJ Full. Similarity in multilegged locomotion: Bouncing like a monopode. *Journal of Comparative Physiology A: Neuroethology, Sensory, Neural, and Behavioral Physiology*, 173(5):509–517, 1993.
[31] J.G.D. Karssen and M. Wisse. Running robot phides. *Dynamic Walking*, 2012.
[32] M.H. Raibert. *Legged robots that balance*, volume 1. The MIT Press, 1986.
[33] S. Kajita and K. Tani. Study of dynamic biped locomotion on rugged terrain-derivation and application of the linear inverted pendulum mode. In *Robotics and Automation, 1991. Proceedings., 1991 IEEE International Conference on*, pages 1405–1411. IEEE, 1991.
[34] T. Koolen, T. de Boer, J. Rebula, A. Goswami, and J. Pratt. Capturability-based analysis and control of legged locomotion, part 2: Application to three simple gait models. *In Print*, 2011.

Chapter 2

Running over obstacles

Running over obstacles

Literature Study

Niels van der Geld

Advisor: Daniël Karssen

August, 2011

Delft University of Technology Delft Biorobotics Laboratory, 3mE

Abstract

State of the art running robots can handle small floor height disturbances, but cannot run over rough terrain. A reason for this is that most running robots only react to perturbations, but not anticipate to these perturbations. In this paper, we present an overview about what is known in literature about how robots and humans anticipate to obstacles. It is known when humans detect an obstacle, how they adjust their steps and where last foot prior to overstepping is positioned. However, it is unknown at what moment and how humans start to alter their stride, but clues are given by long jumping related studies. For robots are methods available to adjust the step length and to calculate step locations. Adjustment can be achieved by adjusting gait parameters such as flight phase, stance phase and forward velocity, or by using an asymmetric gait. Currently it is unknown what method disturbs the natural running gait the least.

Contents

Chapter 1

Introduction

Almost all current mobile robots use wheels to move around. Wheels provide an easy to implement and energy efficient way of moving around, but they restrict robots to flat terrain. Legged robots, on the other hand, have the potential to handle non-flat or rough terrain, as they can select their ground contact points.

The current state-of-art legged robots are able to run on a flat terrain and they can cope with small perturbations [1], [2]. However, these robots are not yet able to run over rough terrain. A reason why these robots cannot handle rough terrain is that they only react to perturbations, but not anticipate to these perturbations. Reacting to a perturbation works well for small perturbations, but an anticipative action is needed to handle large perturbations.

For robots it is currently unknown how to anticipate to large perturbations. In this paper, we present a literature study about what is known about how robots and humans anticipate to obstacles. We study besides robots, also humans, because human related studies provide useful clues about how to cope with such a situation. Bipedal robots are studied as they also provide information about how humans walk, run and anticipate to perturbations.

The goal of this paper is to determine the best method to cope with an obstacle in the horizontal plane for a 2D running biped, while disturbing the natural running gait the least.

This literature study will only cover obstacle avoidance in the sagittal plane (2D) to give the best overview possible of overstepping methods. In order to understand the goal of this paper, it is important to know what is defined as an *obstacle*. Normally one can cope with an obstacle in three ways. The first way is stepping *around* the obstacle, the second way is stepping *on* the obstacle and the third way is stepping *over* the obstacle.

In this literature study, the obstacle is defined as having infinite width. Note this constraint makes motion-planning papers not interesting for this study, as their focus is mostly about avoiding the obstacle by going around it. Further, the obstacle is defined as an area in the xy-plane with a variable height, i.e. like a step-up or a gap. Therefore, the focus will be on stepping over an obstacle. Figure 1.1 shows a graphical representation of possible obstacles.

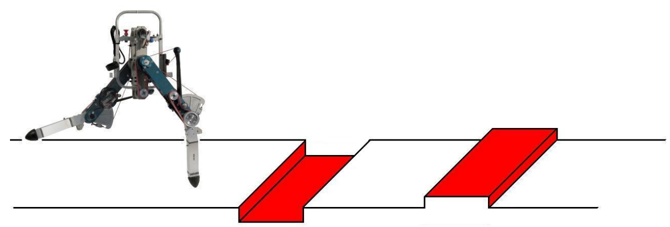

Figure 1.1: Graphical representation of two obstacles, showing a gap and a step-up. The robot is not able to run outside the lane, suggesting the infinite width of the obstacles.

Chapter 2 discusses the results found in literature for human obstacle avoidance. When a human runner approaches an obstacle, there is a sequence of acts enabling the human to overstep an obstacle. These acts are divided into four categories, in order to give a clear overview. Chapter 2 discusses these categories by section. Chapter 3 discusses the results found in literature for robots. Obstacle detection for robots is not covered in this literature study, as this topic has been covered in other studies [3], [4] and suitable methods to detect obstacles are available. Chapter 3 will discuss methods for step adjustment and footstep locations. Chapter 4 discusses the conclusions of this literature study and related future work.

Chapter 2

Human Obstacle Avoidance

Introduction

What do humans do when they want to overstep an obstacle or gap? This chapter gives an overview about what is known in literature about human obstacle overstepping. The information gained from human obstacle overstepping can be used in the design of a robot obstacle-overstepping algorithm. When a human oversteps an obstacle, there is a sequence of acts. These acts can be divided into four categories:

I: Moment of obstacle detection while moving.

II: Position of the last foot prior overstepping the obstacle.

III: Step location planning between the point the obstacle is detected and the object.

IV: Methods for step adjustment.

In literature, we found several papers about the acts of categories I, II and IV, but none papers about step location planning, category III. However, we found a number of papers about step location planning used by long jumpers. The found papers for each of these categories are discussed in the following sections.

2.1 Obstacle Position Detection

When do humans start to look at an obstacle, and how important is visual information for obstacle overstepping? It is shown by Patla et al. [5], that humans start to gaze at the obstacle in the 4 - 6 meter region when humans approach an obstacle. Adult humans have a step length of approximately 70 *cm* [6], and so the gazing behaviour starts approximately 6 to 9 steps away from the obstacle.

Is knowing the whereabouts of the obstacle in advance enough to overcome the obstacle successfully? Patla et al. [7] shows that visual information is important to overcome an obstacle. In this study, subjects were allowed to look at the obstacle in advance, but not during the last 5 or 6 steps. This caused subjects to trip over or step on the obstacle, hereby showing that visual information acquired about the obstacle in advance is not enough to avoid the obstacle.

Apparently, humans need more feedback to overstep obstacles successfully. However, when do humans need to detect an obstacle to achieve a successful overstep? Regarding their gazing behaviour, humans look at their footsteps prior overstepping the obstacle according to Patla et al. [8]. Humans look the last two steps before the obstacle at their feet, to see the relation between their feet and the obstacle and to ensure no collision between their feet and the obstacle occurs. Hereby it can be concluded that precise step planning or foot placement in the approach to the obstacle is not important except for the last two steps. This is supported by a study done by Mohagheghi et al. [9], which shows that successful obstacle avoidance is possible provided visual information is available at least two steps before the obstacle.

Discussion

Patla wrote that people start gazing at an object at a range of 4 - 6 meter and only fixate on their footprints two steps before avoiding an obstacle. Patla also states that people really focus on their footsteps the lasts two steps before the obstacle and Mohagheghi shows that with visual information successful overstepping can be realized within just two steps. It can be concluded that one can start altering their gait, while walking, anywhere between 9 and 2 steps to successful overcome an obstacle. However, it is shown that the largest changes are made in the last steps prior to overstepping.

2.2 Foot-Obstacle Position

While approaching an obstacle, where should the last foot prior to overstepping be positioned? Depending on the obstacle, the optimal position to place the last foot before the obstacle differs per situation. There are two obstacle possibilities: (1) the obstacle is an area where one is not allowed to place a foot, like a gap, or (2) the obstacle has a certain height. Figure 1.1 shows a graphical representation of both these situations.

In the first situation (1), the location of the foot depends on the size of the gap or area. In a situation in which the length of the obstacle is overstep-able with a normal step, than step adjustment might be required. It can be deducted that the location of the last foot should be as close to the edge as possible. Placing the foot closer to the edge allows stepping over a bigger gap with a normal step.

An example can be the 'obstacle' for long jumpers. For the long jumper, the goal is to achieve the biggest step length possible. In order to do this, the long jumper places his last foot on the edge of the obstacle, the bar in the floor [10]. Therefore, if the length of the obstacle is uncertain, but it is known that the obstacle can be overstepped with a normal step, than the position of the last foot should be as close to the edge as possible. This improves the chances of overstepping the obstacle successfully.

In the second situation, if the height of an obstacle is non-zero (2), it is not preferable to place the foot as close to the edge as possible. To maintain a smooth gait while crossing the obstacle, the foot is placed further before the obstacle according to Sparrow et al. [11]. It was found that the crossing distance, expressed as a percentage of the normalized step length at which the obstacle is crossed, remains almost unchanged with obstacle height as can be seen in figure 2.1. The same result is found in a study done by Berard et al. [12]. For male subjects this is around 80% of the step length, and for female subjects this is around 75% of the step length, both for their lead leg. Sparrow also found, that with increasing obstacle height the duration of lifting the leg over the obstacle increases and the velocity lowers. This can be seen in figure 2.2.

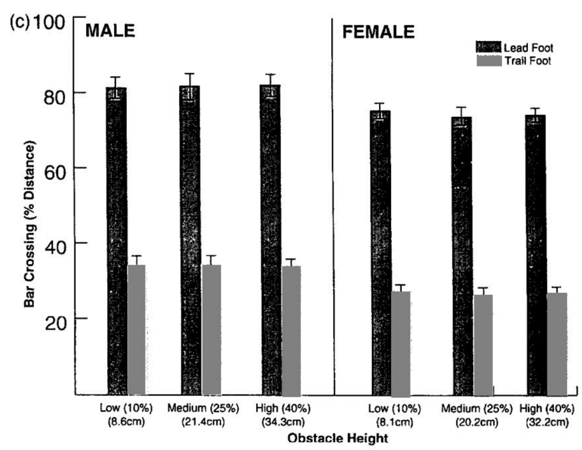

Figure 2.1: Reprint from [11]. Bar crossing distance, for male and female subjects. With crossing distance % per step length.

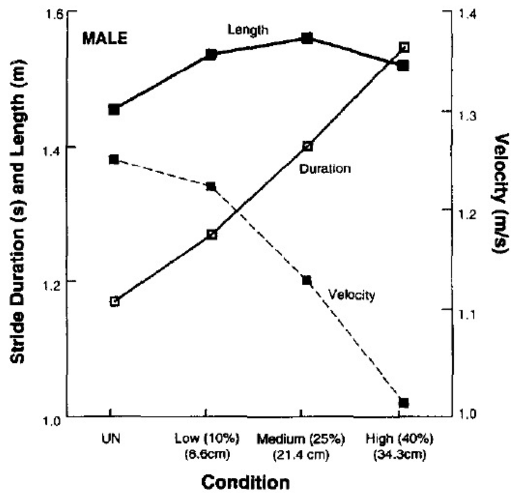

Figure 2.2: Reprint from [11]. Stride characteristics for male adults for unconstrained walking (UN) and for crossing an obstacle of height 10%, 25% and 40% of leg length.

Discussion

Sparrow's and Berard's studies show that the position of the last foot before the obstacle, is at a constant distance from the obstacle. However, it is unclear what happens if the height of the obstacle goes to 0. When the height lowers, the situation goes from (2) to (1), ending up with an obstacle like long jumpers have. The result found in Sparrow's and Berard's study is in such a situation questionable.

2.3 Step Location Planning

Although it is known when humans detect an obstacle, at what distance related to the obstacle do humans start to alter their gait? In order to develop a step adjustment controller, it can be useful to know at what moment humans start to alter their gait, and in what manner the gait is altered. For normal running humans, currently no studies have been done on this topic. However, some clues are given by studies of step location planning in long jumping.

Lee et al. [10] found that long jumpers divide their run-up to the board in two phases; an initial accelerative phase, ending about 6 m from the board, and the second phase, where the jumpers adjust their stride pattern. This matches the findings of Patla [5], where subjects started to look at the obstacle from about 6 m and subsequently started to alter their stride. It can be concluded that the obstacle is detected in the same distant range. Hay et al. [13] show the same results about the two phases. They also conclude that the last gait adaptions are done in the last two steps of the run up and that regulating the vertical impulse is used to achieve step length adjustment.

Montagne et al. [14] showed that the second phase of the long jumper's approach was initiated between the $6th$ and last step. Experiments showed that the regulation was more often initiated at the second-to-last (22.58%), the third-to-last (29.03%), or the fourth-to-last step (17.74%). A linear regression analysis on the amount of adjustment and the step number at which regulation was initiated showed that the greater the amount of adjustment, the earlier the regulation was initiated. This can be seen in be seen in figure 2.3.

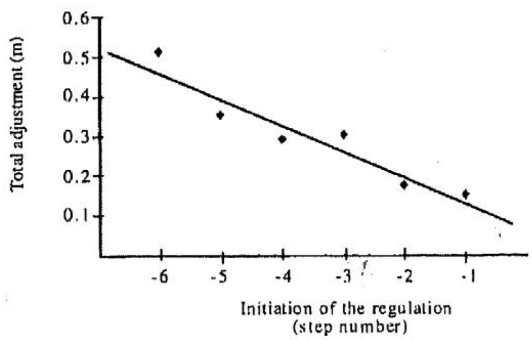

Figure 2.3: Reprint from [14]. The amount of adjustment (m) as a function of the step number at which regulation was initated. The linear regression analysis showed that the higher amount of adjustment, the earlier the regulation was initiated.

Discussion

The studies done about long jumping, show that long jumpers divide their run-up in two sections. The second phase is used to alter the step planning to get the last foot to the edge of the object as close as possible. This phase gives clues about how human plan their step locations. However, the run-up to a long jump is different from regular running, as is the goal of the 'obstacle' to overcome. It is unclear to what degree the clues found for long jumping can be compared to normal running step location planning.

2.4 Step Length Adjustment

According to the previous section it is not known what drives humans to determine their footholds prior to overstepping an obstacle. But what do humans prefer in adjusting their step length? This section shows that humans do prefer lengthening their step. This might help to deduct how humans determine their footholds between themselves and the obstacle.

Patla et al. [15] did a study towards the decision whether to make a longer step or a shorter one. In this study, lights visually cued subjects, indicating available stepping positions. It was found that 50% of the subjects responded by increasing their step length, whereas 30% responded by decreasing their step length. The success rate was lower for later cueing times and it was lower for shorter step length than for longer step length. Patla suggests that balance requirements constrain the adaptations that can be made, so it depends at which moment during the gait the subject would be disturbed. Lengthening does occur more, however, there are situations where shortening is preferred. Experiments for both walking and running were done, and the results found were similar.

In order to study alternative step location preferences of humans, Patla et al. [16] did an experiment where subjects were not allowed to step on a lightened spot. The subjects were able to see the spot, and step over, or step around it. There were three major selection methods found: placing the foot in the plane of progression, choosing to take a longer step over a shorter step, and selecting an inward rather than outward foot placement. During the experiment, the subjects knew where the object was, and therefore could alter their step planning to it. Patla proposes that individuals minimize the displacement of the foot from its normal landing spot. Patla's proposal describes the possible positions as vectors, see figure 2.4. The vector starts at the original landing position of the swing foot, and ends at the possible new position of the swing foot. This would result that an inward or outward foot placement would be preferred above step lengthening, because the vector length is shorter. However, it was found by experiments that step lengthening was preferred above an inward movement, and it was hypothesized that a movement inwards would cost more effort than step lengthening. Selecting a step sideways is not relevant for this literature study, as the obstacle was defined having infinitive width, so this option is ignored. Furthermore, step lengthening is preferred above shortening, as shortening requires reduction in the forward momentum of the body.

Step adjustment behaviour of humans about suddenly appearing obstacles has been studied by Weerdesteyn et al. [17]. In this study, the subjects walked on a treadmill, schematic diagram of the setup can be seen in figure 2.5. The subjects were only allowed to step *over* the object, which was dropped onto the treadmill in front of the left foot. This forced the subjects to make a decision between making a long step, or a short step to overcome the obstacle. The choice of step strategy varied on the available time for response and did not alter the rest

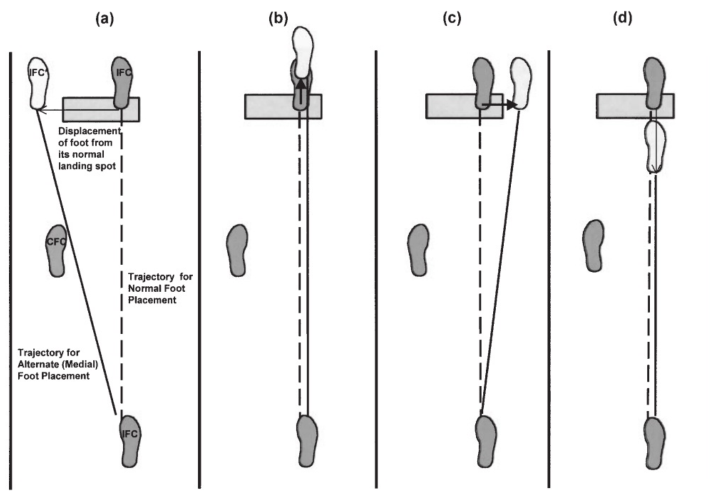

Figure 2.4: Reprint from [16]. A schematic diagram showing how the magnitude of foot displacement from its normal landing spot to four possible choices can be used to determine the new swing-limb trajectory through vector summation. Normal swing-limb trajectory is shown as dashed lines. (b)-(d) shows the three option avoid an obstacle, step lengthening (b), step sideways (c) and step shortening (d).

of the step strategy. Reaction time on step lengthening or shortening did not significant differ, but lengthening occurred more. This could be due to that the momentum causes the body to move on, and performing a counteraction would take more effort and time.

In order to investigate whether lengthening or shortening of the step has the preference, Weerdestyn et al. [18] proposed to use the minimisation of displacement theory. This theory states that minimisation of displacement of the foot from its original landing position has to be the main criterion for the selection of alternative foot placement. For each trial, it was calculated how much lengthening and how much shortening of the stride was required minimally for successful avoidance. This results in a vector, starting from the original landing spot of the foot to the new landing spot. See figure 2.6. This is the same method Patla [16] used. With experiments was shown that the behaviour of younger women was in agreement with the minimal displacement criterion, whereas the older women would prefer the longer step, even when shortening of the step would be the more obvious choice. This could be explained by the fact that taking a longer step over a short step is possibly less destabilizing and could result in a standstill, whereas a short step could cause tumbling over. This is the same conclusion that Patla et al. [16] draws. However, this is in contradiction with

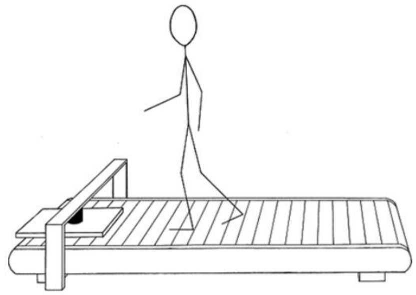

Figure 2.5: Reprint from [17]. Schematic diagram of the experimental setup. The electromagnet (colored black) is attached to a bridge over the front of the treadmill. After a trigger from the computer has switched off the electromagnet, the obstacle falls onto the treadmill in front of the participant his left foot.

the results found by Chen et al. [19], they found that older adults prefer shortening their step. Differences could be caused by different experimental setups. Chen used a band of light, which was always visible. Weerdesteyn used a setup with a treadmill, similar to a previous study [17], as can be seen in figure 2.5.

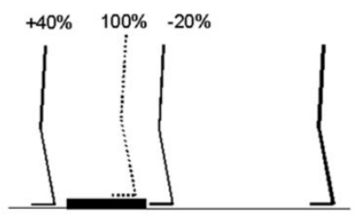

Figure 2.6: Reprint from [18]. Calculation of Δ-step-strategy (Δ-SS). The dotted stick figure represents the normal landing position. In this example, 20% shortening or 40% lengthening would be required in order to avoid the obstacle successfully. The difference between lengthening and shortening (Δ-SS) is 20% in favor of shortening.

Rietdyk et al. [20] studied the modifications in gait parameters for long jumping in several situations. To achieve a single lengthened step, runners decreased braking and increased push-off during stance, and increased the reach of the swinging leg. When foot placement was also important for the second subsequent step, than the gait parameters were modified in both stance and swing legs during the first step. If a short step followed the long step, the center of mass was moved backwards in the first step. With two long steps, the take-off velocity was increased, while the landing velocity was reduced.

Discussion

Most studies show that lengthening of the step is preferred to overcome an obstacle. There are some exceptions, but these can be seen as a result of a different experimental setup, or different initial conditions. The study done by Rietdyk study shows that altering the step length during running in the approach of a jump is complex and that several parameters are changed differently depending on whether or not foot placement is contained in the next step.

2.5 Conclusion

For overstepping an obstacle, the only part that remains unknown is how humans plan their steps between them and the obstacle. For long jumpers clues are given about how they alter their steps, but it is unknown to what degree this is equal to normal running humans. Because of this uncertainty, there is no conclusive number of control methods. However, two major control methods can be described. The first strategy involves altering the running gait with the knowledge of an obstacle being present that needs to be overstepped in a certain distance range. Altering step planning can start in the range of 6 to 9 steps to overstep the obstacle. The second strategy will be more drastic, being able to control the steps in such a way that one is able to overstep a suddenly appearing obstacle in just 2 or 3 steps. In addition, it should be noted that a transition moment should be implemented: when to switch between the two methods?

In order to achieve full insight in human obstacle avoidance, actual step location planning should be studied for walking and running humans. Currently only clues are given by results found for long jumpers and the preferences of step length adjustment.

Chapter 3

Robotic Obstacle Avoidance

Introduction

In this chapter, an overview is given about the methods and strategies known and used for robots to overcome obstacles. In order to adjust the steps of the robot to overstep the obstacle, two main questions have to be answered: *where* to place the feet of the robot and *how* to adjust the steps of the robot to get the feet on the right location. The first section will answer the question *where* to place the feet of the robot during its gait. The second section will answer the question *how* to adjust the step planning. Each section is followed by a discussion.

The previous chapter discusses the position detection of the obstacle for humans. For robots, it is possible to use cameras in order to monitor objects and pattern recognition programs can be used to gain information about these objects. The Honda Asimo [21] robot does have a system like this, but also the robot TULip from the TU Delft [22] features such cameras. Obstacle detection is not included in this literature study, as this topic has been covered in other studies [3], [4].

There are two major different walking techniques: (1) Zero Moment Point (ZMP) walking [23], like the Honda Asimo [21] and (2) dynamic walking. However, ZMP robots might use interesting methods, so papers regarding ZMP related methods also taken into account.

3.1 Step Locations

In the process of letting the robot cope with an obstacle, it is known that detecting of an obstacle is possible. But how to determine where to place the feet of the robot, in order to get to the obstacle? This section will discuss first where to place the last foot before the obstacle, followed by methods for foot step location.

In the section about how humans position their last foot prior to overstepping the obstacle, there are two obstacle possibilities defined: (1) the obstacle is an area where one is not allowed to place a foot, like a gap, or (2) the obstacle has a certain height. The same holds for robotic obstacle overstepping.

For obstacles with zero or negative height (1) it is preferable to place the foot as close to the edge as possible according to Nieuwenhuizen [24]. Nieuwenhuizen states that the error in distance estimation increases as the distance to the object increases. If the length of the obstacle is uncertain, but it is known that the obstacle can be overstepped with a normal step, than the position of the last foot should be as close to the edge as possible.

For obstacles with a positive height (2), the step location can be calculated if the exact location and height of the obstacle are known. Yasar et al. [25] developed a system to overstep an obstacle with height. They chose in their experiments to take a full-length step while overstepping an obstacle, even if the size of the obstacle was smaller. This is because computation of different stepping trajectories for stepping over obstacles of different sizes would make the algorithm more computationally complex. For experiments, they used a ZMP robot, which is able to stop before the obstacle and to balance itself in double support state before overstepping the obstacle. The algorithm propesed by Yasar et al. successfully demonstrates a global reactive footstep planning method with a human-like approach.

Dittrich et al. [26] showed that obstacle avoidance in bipedal robots can be achieved with sensory feedback and closed loop control. Using a robot based on the SLIP model with linear leg retraction, periodic stable running was approached. No information about the location of the obstacle was put into the system, but by controlling the angle of attack of the leg, hopping over and on obstacles was achieved. Hodgins et al. [27], [28] showed with experiments, that they are able to let the robot step on a desired target. Simply put, if the location of the obstacle is known, than by backwards calculating it is possible to determine the footstep locations for the robot. In this experiment, the footstep locations were only calculated once, and not iterated. With this method, successful jumping over obstacles was achieved as well. The distance between the footstep locations were chosen to be as close to the original running gait as possible to minimize differences in step length.

Lewis et al. [29] showed that it is possible to achieve human-like overstep behavior over an obstacle by using just a few image samples of the environment prior to overstepping an obstacle. Patla et al. [30] showed, that humans can walk with intermittent visual sampling. Successful overstepping depends on the sampling moment. According to Hollands et al. [31], samples taken when the foot to be controlled is in stance phase are far more effective in modulating gait than samples taken in swing phase. For the experiments by Lewis et al., a range encoder was used to estimate the distance to the obstacle in the last three steps before the obstacle. By using a learning algorithm, they managed to alter the gait of the robot smoothly, to overstep the obstacle. It was shown that the step length of the robot is gradually changed to overstep the obstacle, see figure 3.1.

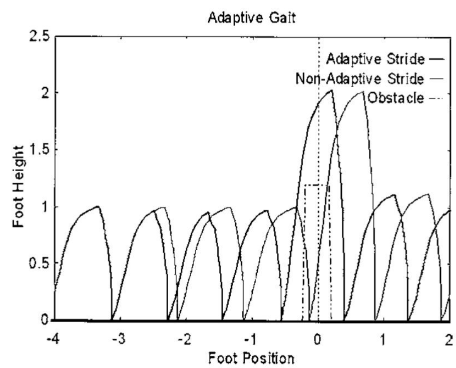

Figure 3.1: Reprint from [29]. Examples of gait trajectory before and after learning. The foot goes through the obstacle, as no attempt was made to simulate the physics of the foot's collision with the obstacle.

Discussion

The study done by Yasar et al. contained a ZMP robot, which was stopped prior to overstepping the obstacle. This made it possible to overstep the obstacle in the most efficient way. However, this method does disturb the natural running gait completely. If the goal is to overstep an obstacle with 0 height, the foot can be placed as close to the edge as possible, according to Nieuwenhuizen.

With the methods used by Hodgins et al., it is possible to adapt the running gait of the robot and to successful overstep an obstacle. However, Hodgins et al. only calculated the footstep locations once for the robot and did not iterate it. Humans do not calculate their footstep locations when they see an obstacle. Therefore, Hodgins et al. method could work, but is far from 'human'.

The method proposed by Lewis et al. seems promising for the use with a 2D running robot. An obstacle can be programmed into the learning algorithm, and it could be tested whether or not it also works for running robots. Simulations could tell whether this would work with a dynamic robot.

3.2 Step Adjustment Methods

In order to overstep an obstacle, the robot needs to adjust the length of its step. However, how is step length adjustment achieved? This section will discuss the methods available for step adjustment. The focus is on step lengthening and shortening, as these are the only possible options to overstep the obstacle of infinitive width.

A method used to achieve different step lengths is proposed by Yagi et al. [32]. They proposed a control strategy for a ZMP robot that made it possible to avoid obstacles by going around, over, or stepping on them. The strategy consists out of several preprogrammed solutions like different step lengths that are stored and used to achieve the optimal position to avoid the obstacle. Although the ZMP robot used for experiments is successfully able to deal with scenes and unknown obstacles, it is not known if preprogrammed solutions work for a dynamical walking robot.

For dynamic running robots, Hodgins et al. [27] proposed three methods to control step length: adjusting the duration of flight phase, the duration of stance phase, or variation in the forward velocity, see figure 3.2 for a graphical representation. Experiments showed that adjusting flight duration and adjusting forward velocity, produce similar accuracy in following a pattern of footholds, but that adjusting forward velocity allows a greater range of step lengths. Furthermore, it was found that changes in stance duration are not large enough to produce a large change in step length.

The step length can also be controlled by the use of an asymmetric gait, according to Dunn et al. [33]. In an asymmetric gait, the two legs have a different gait. In order to achieve smooth walking (where smooth walking is defined as $\mathbf{v}^- = \mathbf{v}^+$, see figure 3.3), they developed an algorithm being able to control the walking speed as a function of the step length. The basis of the algorithm is an asymmetric gait to adjust walking velocity combined with a set of conditions on the leg lengths. The algorithm is able to track independently 30% change in desired walking velocity and a 25% change in desired step length, while maintaining smooth exchange of support.

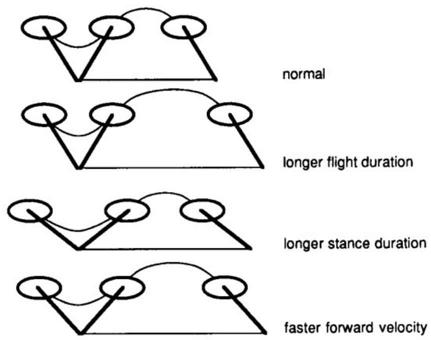

Figure 3.2: Reprint from [27]. The top drawing portrays a normal step. The three other drawings show longer steps produced by the three methods for adjusting step length. The second drawing has an extended flight phase, the third an extended stance phase, and the fourth an increased forward velocity.

Discussion

The method proposed by Yagi et al. with preprogrammed solutions seems logical for ZMP robots, as their computations are complex. For dynamic walkers it is the question whether or not this is the optimal solution. Dynamic walkers have due to their control technique often different initial conditions prior to their next step and preprogrammed solutions could result in a non-stable gait. The methods proposed by Hodgins et al. and Dunn et al. seem usable. A possible combination of both methods might lead to flexible and usable solutions in adjusting the step length. Experiments in simulations and on the real robot should give insight in this. It should be noted that both experimental robots

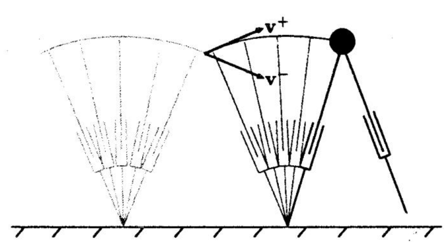

Figure 3.3: Reprint from [33]. During single support, the hip follows the arc of a circle with radius equal to the stance leg length. At exchange of support, there is an instantaneous change in linear velocity of the hip. In order to achieve smooth walking, vector $\mathbf{v}^-$ should be equal to vector $\mathbf{v}^+$, which is not achieved in this figure.

used by Hodgins and Dunn feature legs without knees. If these methods work on kneed robots is currently unknown.

3.3 Conclusion

Successful overstepping of an obstacle is theoretical achievable. The location of the last foot prior to overstepping depends on the obstacle and step length adjustment is achievable by altering the gait parameter of the robot. Whether the methods proposed by Hodgins et al., the method proposed by Dunn et al., or a combination of both are favored could be decided by the means of simulation or experiments. The footstep locations can be calculated, and therefore successful overstepping is possible. Human-like footstep planning can be achieved, although it is not known how humans exactly plan their foot steps. However, the study done by Lewis gives a useful clue in how humans would act in order to overstep an obstacle.

Chapter 4

Conclusion

This literature study gives an overview on what is know about how humans and robots overstep obstacles. In order to develop a step planning controller for a 2D running robot, available methods are compared and tested whether they match with the goal of this study, which is to determine the best method to cope with an obstacle in the horizontal plane for a 2D running biped, while disturbing the natural running gait the least.

It was found that humans detect an obstacle in the 6 m region, and from that point they are therefore able to adjust their step planning. However, when humans exactly start to alter their gait, and how, is currently unknown. For long jumpers clues are given about how they alter their steps, but it is unknown to what degree this is equal to normal running humans. Long jumpers make their final adjustments *mostly* in the last two steps of the run up, by controlling their vertical impulse. This gives insight in when humans adjust their steps, but no exact results are known as no studies have covered this topic. Because of this uncertainty, there is no conclusive number of control methods. This makes it therefore impossible to develop a step length controller for a robot which is inspired on human behavior. For step length adjustment, it is shown that step lengthening has the preference, although shortening does occur.

For robots is it possible to create a controller, which is able to adjust the gait of the robot in such a fashion that the robot can overstep an obstacle. Obstacles can be detected or can simply be programmed in the control algorithm. Step adjustment and planning can be realized by the methods proposed by Hodgins and Dunn. In simulations can be experimented in to what degree the methods match the research question by disturbing the natural running gait the least.

But does any relation exist between current studies about human and robotic obstacle overstepping? In experiments done by Hodgins et al., the robot started to alter its gait 5 m in advance of the obstacle. This matches results found by Patla et al., where subjects started to gaze at an obstacle in the $4 - 6$ m region and subsequently started to alter their gait. However, Hodgins et al. did a backwards calculation to determine equal step lengths for the robot, while for humans it was found that humans mostly make their final adjustments in the last two steps. So obstacles can be overstepped, but the method used by Hodgins et al. is not human-like. The method used by Lewis et al. does provide an iterative adjustment method, which seems more human-like, but this method was not tested for running nor dynamic walking robots. Information about step location planning and step adjustment methods is provided in studies about long jumping, however it is not known to what degree this can be compared to normal human running. Therefore it can not be said if this information can be used to determine the best method to cope with an obstacle in the horizontal plane for a 2D running biped, while disturbing the natural running gait the least.

4.1 Future work

We would like to recommend that actual step location planning for humans should be studied. This is in order to develop a controller to achieve successful step location planning in a human-like way. Furthermore, it should be studied to what degree the run-up and the adjusting behavior of long jumpers can be compared to normal running and adjusting of humans.

The step length adjustment methods proposed by Hodgins et al. and Dunn et al. should be tested whether or not they perform well on kneed robots. Furthermore, combining the proposed methods might lead to flexible controllers, although this has not be done yet. In the introduction was mentioned that a measure should be found to compare initial running gait with the adapted gait for overstepping the obstacle. This measure needs to be found, in order to determine the best step length adjustment method.

Bibliography

[1] R. Tajima, D. Honda, and K. Suga. Fast running experiments involving a humanoid robot. In *Robotics and Automation, 2009. ICRA'09. IEEE International Conference on*, pages 1571–1576. IEEE, 2009.

[2] R. Niiyama, S. Nishikawa, and Y. Kuniyoshi. Athlete robot with applied human muscle activation patterns for bipedal running. In *IEEE-RAS International Conference on Humanoid Robots (Humanoids 2010)*, pages 498–503, 2010.

[3] P. Jonker, J. Caarls, and W. Bokhove. Fast and accurate robot vision for vision based motion. *RoboCup 2000: Robot Soccer World Cup IV*, pages 149–158, 2001.

[4] M.D. Adams. Lidar design, use, and calibration concepts for correct environmental detection. *Robotics and Automation, IEEE Transactions on*, 16(6):753–761, 2000.

[5] A.E. Patla and J.N. Vickers. Where and when do we look as we approach and step over an obstacle in the travel path? *Neuroreport*, 8(17):3661, 1997.

[6] M. Whittle. *Gait analysis: an introduction*. Butterworth-Heinemann Medical, 2002.

[7] A.E. Patla and M. Greig. Any way you look at it, successful obstacle negotiation needs visually guided on-line foot placement regulation during the approach phase. *Neuroscience letters*, 397(1-2):110–114, 2006.

[8] A.E. Patla and J.N. Vickers. How far ahead do we look when required to step on specific locations in the travel path during locomotion? *Experimental Brain Research*, 148(1):133–138, 2003.

[9] A. A. Mohagheghi, R. Moraes, and A.E. Patla. The effects of distant and on-line visual information on the control of approach phase and step over an obstacle during locomotion. *Experimental Brain Research*, 155(4):459–468, 2004.

[10] D.N. Lee, J.R. Lishman, and J.A. Thomson. Regulation of gait in long jumping. *Journal of Experimental Psychology: Human Perception and Performance*, 8(3):448–459, 1982.

[11] W.A. Sparrow, A.J. Shinkfield, S. Chow, and R.K. Begg. Characteristics of gait in stepping over obstacles. *Human Movement Science*, 15(4):605–622, 1996.

[12] J.R. Berard and L.A. Vallis. Characteristics of single and double obstacle avoidance strategies: a comparison between adults and children. *Experimental brain research*, 175(1):21–31, 2006.

[13] J.G. Hay and H. Nohara. Techniques used by elite long jumpers in preparation for takeoff. *Journal of biomechanics*, 23(3):229–239, 1990.

[14] G. Montagne, S. Cornus, D. Glize, F. Quaine, and M. Laurent. A perception-action coupling type of control in long jumping. *Journal of Motor Behavior*, 32(1):37–43, 2000.

[15] A.E. Patla, C. Robinson, M. Samways, and C.J. Armstrong. Visual control of step length during overground locomotion: task-specific modulation of the locomotor synergy. *Journal of Experimental Psychology: Human Perception and Performance*, 15(3):603–617, 1989.

[16] A.E. Patla, S.D. Prentice, S. Rietdyk, F. Allard, and C. Martin. What guides the selection of alternate foot placement during locomotion in humans. *Experimental Brain Research*, 128(4):441–450, 1999.

[17] V. Weerdesteyn, B. Nienhuis, B. Hampsink, and J. Duysens. Gait adjustments in response to an obstacle are faster than voluntary reactions. *Human movement science*, 23(3-4):351–363, 2004.

[18] V. Weerdesteyn, B. Nienhuis, T. Mulder, and J. Duysens. Older women strongly prefer stride lengthening to shortening in avoiding obstacles. *Experimental Brain Research*, 161(1):39–46, 2005.

[19] H.C. Chen, J.A. Ashton-Miller, N.B. Alexander, and A.B. Schultz. Age effects on strategies used to avoid obstacles. *Gait & Posture*, 2(3):139–146, 1994.

[20] S. Rietdyk and A.E. Patla. Does the step length requirement in the subsequent step influence the strategies used for step length regulation in the current step? *Human Movement Science*, 13(1):109–127, 1994.

[21] Y. Sakagami, R. Watanabe, C. Aoyama, S. Matsunaga, N. Higaki, and K. Fujimura. The intelligent ASIMO: System overview and integration. In *Intelligent Robots and Systems, 2002. IEEE/RSJ International Conference on*, volume 3, pages 2478–2483. IEEE, 2002.

[22] D. Hobbelen, T. de Boer, and M. Wisse. System overview of bipedal robots flame and tulip: Tailor-made for limit cycle walking. In *Intelligent Robots and Systems, 2008. IROS 2008. IEEE/RSJ International Conference on*, pages 2486–2491. IEEE, 2008.

[23] M. Vukobratovic and B. Borovac. Zero-moment point-thirty five years of its life. *International Journal of Humanoid Robotics*, 1(1):157–173, 2004.

[24] N. van Nieuwenhuizen and M. Wisse. Step-over behaviof for limit cycle walkers. *MSc. Thesis Mechanical Engineering - Delft University of Technology*, 2009.

[25] A. Ayaz, K. Munawar, M.B. Malik, A. Konno, and M. Uchiyama. Human-like approach to footstep planning among obstacles for humanoid robots.

[26] E. Dittrich, H. Geyer, A. Karguth, and A. Seyfarth. Obstacle avoidance in a simple hopping robot. *Climbing and Walking Robots*.

[27] J.K. Hodgins and M.H. Raibert. Adjusting step length for rough terrain locomotion. *Robotics and Automation, IEEE Transactions on*, 7(3):289–298, 2002.

[28] J. Hodgins. Legged robots on rough terrain: experiments in adjusting step length. In *Robotics and Automation, 1988. Proceedings., 1988 IEEE International Conference on*, pages 824–826. IEEE, 2002.

[29] M.A. Lewis and L.S. Simo. Elegant stepping: A model of visually triggered gait adaptation. *Connection Science*, 11(3):331–344, 1999.

[30] A.E. Patla, A. Adkin, C. Martin, R. Holden, and S. Prentice. Characteristics of voluntary visual sampling of the environment for safe locomotion over different terrains. *Experimental brain research*, 112(3):513–522, 1996.

[31] M.A. Hollands and D.E. Marple-Horvat. Visually guided stepping under conditions of step cycle-related denial of visual information. *Experimental brain research*, 109(2):343–356, 1996.

[32] M. Yagi and V. Lumelsky. Biped robot locomotion in scenes with unknown obstacles. In *Robotics and Automation, 1999. Proceedings. 1999 IEEE International Conference on*, volume 1, pages 375–380. IEEE, 2002.

[33] E.R. Dunn and R.D. Howe. Foot placement and velocity control in smooth bipedal walking. In *Robotics and Automation, 1996. Proceedings., 1996 IEEE International Conference on*, volume 1, pages 578–583. IEEE, 2002.